BOSTON UNIVERSITY

COLLEGE OF ENGINEERING

Thesis

MODELING OF DOPANT DIFFUSION IN POLYSILICON INCORPORATING EFFECTS OF GRAIN BOUNDARY MOTION

BY

SOUMYA BANERJEE

B.Tech., INDIAN INSTITUTE OF TECHNOLOGY, 1993

Submitted in partial fulfillment of the
requirements for the degree of
Master of Science in Electrical Engineering
1996

Approved by

First Reader : ____

Scott T. Dunham, Ph.D

Associate Professor of Electrical and Computer Engineering.

Second Reader : ____

S. N. Basu, Ph.D

Assistant Professor of Manufacturing Engineering.

Acknowledgment

I would like to express my deepest gratitude for my advisor, Professor Scott T. Dunham, for his guidance and encouragement during the entirety of my graduate work at Boston University. I would also like to thank Professor S. N. Basu for his timely reading of the manuscript and important insights. Thanks are also due to D. Doppalapudi for his valuable help with TEM work.

None of my experimental work would have been possible if not for the excellent facilities at the Integrated Circuit Laboratory and Technology Research Laboratory at MIT. I would like to take this opportunity to thank all members of these laboratories for their help and suggestions.

I am grateful to all my friends and officemates (past and present) especially Fred Wittel, Mitra Navi, Iuval Clejan, Alp Gencer, Gaurav Shah and Anu Agarwal for their help, support and encouragement throughout my stay here.

Abstract

Doped polysilicon thin films are widely used in the semiconductor industry as gate electrodes, emitters, and diffusion sources for shallow junctions. Determination of the diffusion profiles within polysilicon and from polysilicon to silicon is thus of substantial interest. The resulting concentration profiles are complex due to impurity redistribution upon annealing, which is dependent on the microstructure of the polysilicon. Thin polysilicon films typically have columnar grains separated by regions of high defect concentration referred to as grain boundaries. In these grain boundaries, due to the high defect concentration, dopant diffusivity is increased manyfold. Dopant diffusion in polysilicon takes place through parallel processes of diffusion through the grains and through the grain boundaries, resulting in a net higher diffusivity.

We have developed and implemented a model to simulate dopant diffusion in polysilicon. We have observed that a model based on fixed grain size and dopant incorporation into the grain boundaries just by lateral diffusion of dopants within the grain is insufficient to account for experimental results. From our simulation results, we have concluded that the dominant mechanism of dopant transfer to the grain boundaries is grain growth during which the grain boundaries collect dopants as they sweep across grains. The effects of grain growth have been incorporated into a two stream model which divides the total dopant concentration between the grain and grain boundaries. These two dopant concentrations are coupled by dopant transfer due to grain growth, lateral diffusion of dopants and segregation to the grain boundaries. A transfer rate dependent on grain growth has been used to account for experimental profiles. Experiments have been carried out to further investigate effects of annealing conditions on post-anneal dopant profiles.

Contents

List of Figures

List of Tables

Chapter 1

Introduction

Polysilicon has become a very important material for the very large scale integration (VLSI) era. Understanding and utilization of the advantages offered by polysilicon has been one of the most fundamental developments in the history of integrated circuits. Polysilicon forms an adherent oxide, absorbs and re-emits dopants, has a high melting point, is compatible with hydrofluoric acid (HF), has a compatible work function for metal-oxide-semiconductor (MOS) devices, absorbs heavy metals (gettering), has good step coverage if deposited by chemical vapor deposition (CVD) and forms high conductivity silicides. These properties make polysilicon uniquely suited to be a primary local interconnect material, and its ability to form silicides extends that application to longer interconnect lines. The fact that polysilicon is compatible with integrated circuit processing and it's good step coverage offers many advantages in bipolar and MOS circuits. As a result, polysilicon has many device applications such as self-aligned MOS gates, source/drain contacts, multilayer interconnects, emitter and base contacts and emitter diffusion sources.

As devices sizes continue to shrink, the need to form shallow junctions becomes even more important. An important technique for forming shallow junctions is by diffusion into silicon from a doped polysilicon layer. As a result, understanding the diffusion mechanism in polysilicon as well as being able to predict dopant redistribution under various processing conditions has become very important. During annealing, dopant redistribution in polysilicon is strongly affected by the morphological structure of polysilicon. The polysilicon crystal structure consists of crystalline silicon grains separated by grain boundaries which are fast diffusion paths for the dopant atoms due to the large density of lattice defects. An additional complexity is that the morphological structure of polysilicon changes during annealing, with grains growing in size. This work aims at developing a fundamental understanding of the dopant transport mechanisms in polysilicon and developing a model for the process. The model has been implemented in the process simulator PEPPER using its "dial-an-operator" feature.

Chapter 2 introduces polysilicon as a material and explains in detail the morphology as well as the dopant transport mechanisms in polysilicon. It also explains some of the previous important efforts at modeling dopant diffusion in polysilicon. Chapter 3 deals with our proposed model and Chapter 4 describes the experiments that have been carried out to validate the model. Chapter 5 is a comparison of model predictions to experimental data, and finally Chapter 6 summarizes the work and resulting conclusions.

Chapter 2

Background

2.1 Microstructure and Grain Growth

Polycrystalline silicon consists of grains of crystalline silicon separated by narrow regions of high disorder referred to as grain boundaries. Because of the high defect concentrations in the grain boundaries, dopant diffusivity is increased by at least a couple of orders of magnitude. On the other hand, since the grain interiors are crystalline, dopant diffusivities inside the grain are similar to that in bulk crystalline silicon.

A number of researchers have studied the microstructure of polysilicon as a function of deposition conditions [1, 2, 3]. Lee *et al.* [1] observed that the deposition rate using disilane is faster than that using silane. At the same time, a higher deposition rate leads to a higher transition temperature (temperature at which you get a transition from amorphous to polysilicon) and an increased surface roughness which is undesirable from the point of view of making devices. They also observed that with increasing deposition temperature, the grain diameter decreases and grain density increases owing to the increase in the number of nucleation sites and crystallization rate.

The most popular means of investigating polysilicon microstructure is transmission electron microscopy (TEM) by which various researchers have obtained pictures of the grains in polysilicon both in plan view as well as cross section [3, 4, 5, 6]. TEM micrographs clearly show the cylindrical grains in polysilicon growing from the polysilicon/monosilicon interface upwards. Carrejo *et al.* [7] have carried out scanning tunneling microscopy (STM) to investigate polysilicon grain structure.

TEM measurements require elaborate sample preparation and so are quite time consuming. Scanning electron microscopy (SEM), on the other hand is a simple technique to look at the surface of polysilicon microstructure and requires no sample preparation. However, the resolution and contrasts for SEM are poorer than for TEM and hence grain size measurements are difficult. Bisero has shown that carrying out a chemical etch on the polysilicon samples to delineate the grain boundary facilitates grain size measurement using SEM [8]. He used an etchant comprising of hydrofluoric acid, acetic acid and nitric acid which etches polysilicon by a sequential oxidation-followed-by-dissolution process. The etching rates near grain boundaries and on grain surfaces are different, being more near the grain boundaries. As a result, the contrast between the grain boundaries and the grain increases and SEM measurements of grain sizes is possible. The downside of this process as observed by Bisero is that this process leads to an overestimation of grain sizes.

Grain growth in polycrystalline material has been a subject of interest with many researchers [1, 9, 10, 11, 12, 13, 14]. As expected, when a polycrystalline material is annealed at a high temperature, the grains have been found to grow in size. Grain growth in Si films has been characterized as primary grain growth or secondary grain growth [11, 15]. Primary grain growth occurs when the initial size of the grains is smaller than or on the order of the thickness of the film. Once the grains have grown to a couple of times the thickness of the film, primary grain growth rapidly slows down. Therefore, primary grain growth has been found to be limited by the thickness of the film. In sufficiently thin films, however, after termination of primary grain growth, some particular orientations of grains have been found to keep growing, a process termed secondary grain growth [15, 16]. Secondary grain growth has been found to lead to grain sizes much larger than film thickness with restricted or uniform crystallographic orientations. The rates of both modes of grain growth are affected by the film thickness, impurities, temperature, annealing ambient and deposition conditions.

Grain growth has been observed to be greatly enhanced by the presence of n-type impurities like arsenic and phosphorus while p-type impurities have little or no effect [11, 16, 17]. Since polysilicon films are usually doped, this is a very important factor. It has been observed that phosphorus and arsenic induced enhancement of secondary grain growth can be partially or completely compensated by additional boron doping [11]. This suggests that grain growth enhancement due to the presence of dopants is a Fermi level effect. Further evidence of grain growth being controlled by Fermi level is that for doping concentrations below solid solubility, grain growth rates are equivalent for both phosphorus and arsenic doped material [17].

Mei *et al.* [13] have modeled the enhancement in grain growth due to phosphorus doping as a result of the increase in silicon self-diffusivity, suggesting diffusion or point defect controlled grain growth. Recent studies using high resolution microscopy have revealed that large portions of grain boundaries can be described as periodic arrays of dislocations [18, 19]. Based on these studies, Smith and Tan [20] have suggested that the rate of motion of grain boundary dislocations controls the rate of grain boundary migrations and that the dopants have the same effect on grain growth and dislocation movement. Thus the mobilities of grain boundaries would be expected to depend on the rates of glide and climb of grain boundary dislocations. While glide is a process that does not involve point defects (i.e., it is a non-diffusive process), climb is a diffusive process and requires the movement of point defects.

Kim and Thompson, have proposed a model for grain growth which is based on grain boundary migration as a result of dislocation glide and climb [11]. The rate of normal grain growth can be defined as

$$\frac{dr}{dt} = M \triangle F \tag{2.1}$$

where r is the average radius of the grain, M is the atomic mobility of a grain boundary and $\triangle F$ is the driving force behind grain growth. The driving force for 3-D grain growth is reduction in grain boundary area and can be estimated by

$$\triangle F = \frac{\alpha \, \gamma_{\mathrm{gb}}}{L} \tag{2.2}$$

where γ_{gb} is the average grain boundary energy and α is a constant. Substituting Eqs. 1.2 and 1.3 into Eq. 1.1 and assuming that M is independent of time, Kim and Thompson [11] get

$$L(t)^2 - L(0)^2 = 2 \, \alpha \, \gamma_{\mathrm{gb}} \, M \, t = 2 \, \sigma \, t \tag{2.3}$$

where $L(t)$ represents the diameter after time t and $L(0)$ represents the initial grain diameter. Upon rearranging,

$$L(t)^2 = L(0)^2 + 2 \, \sigma \, t \tag{2.4}$$

This shows that the grain size in polysilicon samples should be growing as the square root of the anneal time. Assuming that the glide and climb processes are additive, with the climb process being dominated by vacancies, it can be shown that [11]

$$\sigma = M \, \alpha \, \gamma_{gb} \left[1 + K \left(\frac{C_V^e}{C_V^i} \right) \right] \tag{2.5}$$

where C_V^e and C_V^i are the total vacancy concentration under extrinsic and intrinsic conditions respectively.

Wada *et al.* [16] carried out grain size measurements in polysilicon as a function of time, temperature and doping level. Mei *et al.* [13] also reported grain sizes in polysilicon and the effect of dopants on grain growth rates. Kim and Thompson carried out extensive experiments to look at grain growth as a function of anneal time and temperature. In all these experiments, samples of polysilicon were doped with phosphorus, arsenic or boron at various concentrations and annealed for different lengths of time over a range of temperatures, and a square root of time dependence of grain growth as shown in Fig. 2.1 was observed.

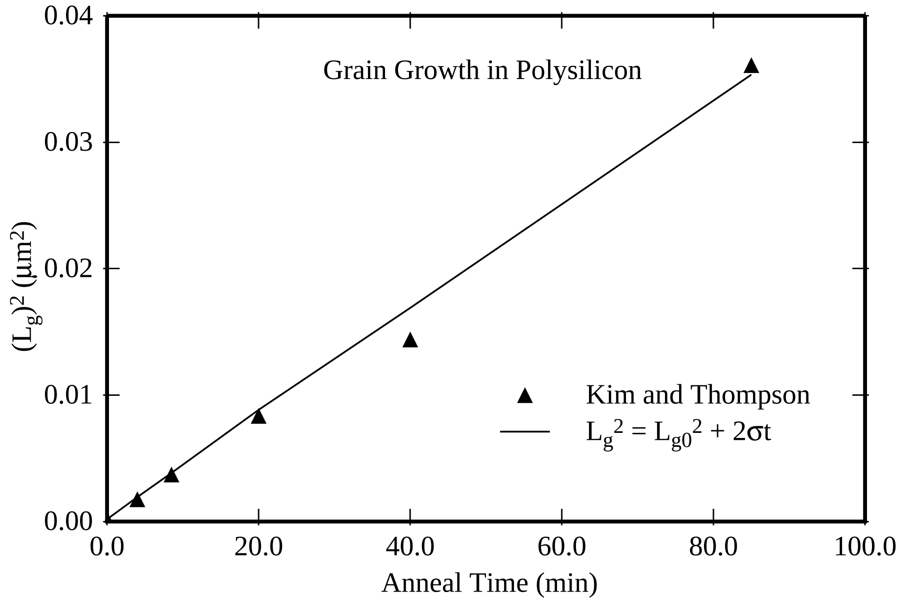

Figure 2.1: Grain growth in polysilicon doped uniformly with $5 \times 10^{20}\mathrm{cm}^{-3}$ of phosphorus and annealed at 950°C [11].

2.2 Segregation to the Grain Boundaries

Investigations have shown that electrical properties of polysilicon are markedly different from those of single crystal silicon [21, 22]. At low dopant concentrations, the resistivity of polysilicon is orders of magnitude higher than monocrystalline silicon and insensitive to changes in dopant concentration. At moderate concentrations, resistivity drops and is very sensitive to changes in dopant concentrations. At high dopant concentrations, the resistivity of polysilicon approaches that of single crystal but always remains slightly higher.

Two primary models have been proposed to explain this variation in resistivity. The carrier trapping model claims that the dopant atoms are distributed throughout the material and resistivity is increased because of carrier trapping at the grain boundaries, where the trapped carriers create potential barriers which impede the transfer of free carriers between the grains [22, 23]. On the other hand, the dopant segregation model suggests that the dopants move into the grain boundaries where they become electrically inactive [24, 25]. Here the variation in resistivity is explained by the hypothesis that at low dopant concentrations, a larger fraction of the total dopants are inactive because of being present in the grain boundary. As the total concentration is raised, more and more dopants are present inside the grains and conductivity approaches that of single crystal silicon.

Both of the above models individually have been able to explain the variation in resistivity with increasing dopant concentration but each has it's own shortcomings. The dopant segregation model is unable to explain the temperature dependence of the film resistivity and the minimum in Hall mobility obtained at intermediate dopant concentrations. On the other side, the carrier trapping model cannot explain the dependence of resistivity on type of dopants.

Mandurah *et al.* [26, 27] have suggested that a combination of both these models may be ideal to explain this phenomenon. Based on their experiments they have tried to characterize segregation of dopants to grain boundaries. They have observed that while arsenic and phosphorus tend to segregate strongly to the grain boundaries, boron does not.

Assuming N_{g} is the concentration in the grain and N_{gb} is the concentration in the grain boundary, Mandurah *et al.* [27] derived the following relationship :

$$\ln\left(\frac{N_{\mathrm{gb}}}{N_{\mathrm{g}}}\right) = \ln\left(\frac{A\,Q_{\mathrm{s}}}{N_{\mathrm{Si}}}\right) + \frac{Q_{\mathrm{o}}}{k\,T_{\mathrm{A}}} \tag{2.6}$$

where A is just a pre-exponential factor, Q_{s} (cm^{-3}) is the density of grain boundary sites, N_{Si} is the total number of both bulk and grain boundary sites, Q_{o} is the heat of segregation, and T_{A} is the temperature. They arrived at this relationship assuming a steady state transfer of dopants from the grains to the grain boundaries with a fixed ratio between the concentration in the grain and the grain boundaries. They also assumed that dopant sites in both the grain boundaries and the grains are far from being saturated.

Mandurah *et al.* [26] implanted polysilicon with different doses of arsenic and annealed the samples at 1000°C for 1 h. They assumed that dopants would be uniformly distributed during this time and grain growth would be stabilized after this anneal so that further low temperature anneal would not lead to substantial grain growth. However as discussed in Chapter 3, both of these assumptions are questionable. They further annealed these samples at temperatures ranging from 800°C to 950°C for times ranging from 64 h to 12 h. Based on these observations, they calculated the pre-exponential factor A and the heat of segregation Q_{o} which they found to vary with the total dopant concentration. Although the variation in Q_{o} observed was small (between 0.44 eV and 0.416 eV), the pre-exponential factor A was found to vary significantly (between 3.02 and 2.17). Fig. 2.2 below shows the variation of the segregation coefficient with temperature as well as with doping concentration as measured by Mandurah *et al.*

Demirlioglu [28] carried out segregation experiments for phosphorus on lines similar to those of Mandurah *et al.* Although Mandurah ignored any grain growth during subsequent low temperature anneals following the initial 1000°C pre-anneal, Demirlioglu carried out her calculations based on the grain size obtained after the lower temperature anneal, instead of the grain size after the pre-anneal. In addition to the differences between phosphorus arsenic, this could explain some of the differences in the parameter values obtained. The value of Q_{o} obtained by Demirlioglu varies in the range between 0.71 eV to 0.77 eV and the value of the pre-exponential factor varies between 0.11 and 0.05.

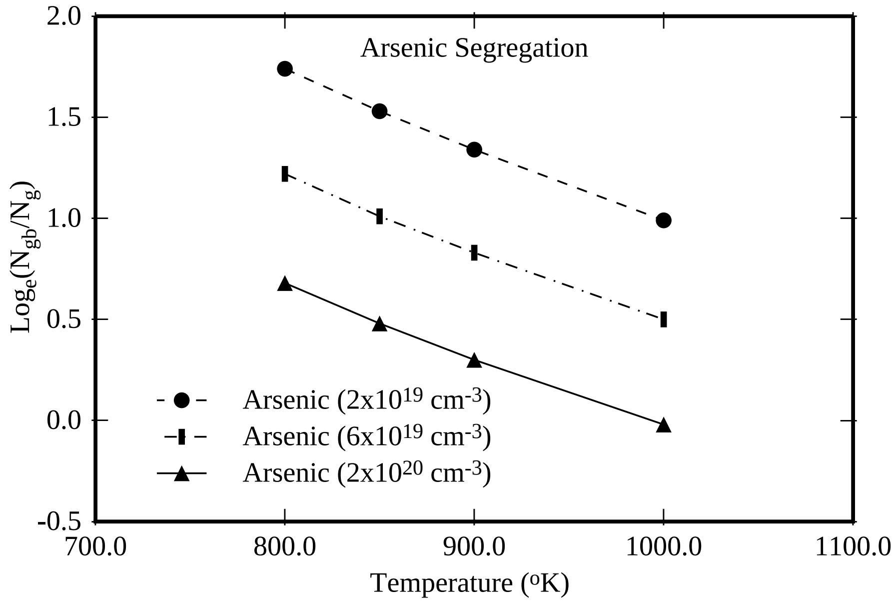

Figure 2.2: Segregation data from Mandurah *et al.* [26].

Another important segregation effect is the segregation of dopants to the polysilicon/monosilicon interface. Traditionally this interface has been considered to be identical to a grain boundary with substantial oxygen content [29, 30]. Sadovnikov *et al.* have observed a dopant pile up at the interface. Luning *et al.* have carried out experiments to determine the segregation of dopants to this interface. One of the goals of this work has been to develop a consistent model and set of parameters for dopant segregation to the grain boundaries and use those results as part of a comprehensive model for dopant diffusion and activation. (See Chapter 3)

2.3 Dopant Diffusion in Polysilicon

Of late various researchers have carried out extensive experiments to look into the technologically important process of dopant diffusion in polysilicon [9, 31, 32, 52, 33, 34]. Experiments carried out are generally of a similar nature varying in deposition conditions, dopant type and concentrations and anneal conditions. Of particular interest is the set of experiments with small thermal budgets carried out by Swaminathan *et al.* [33], since for anneals at high temperatures or long times, doping profiles in polysilicon are generally flat [4, 56]. Swaminathan *et al.* deposited polysilicon by low pressure chemical vapor deposition (LPCVD) on 100 nm of thermally grown oxide atop a <100> silicon substrate, and annealed the undoped polysilicon samples at 1100°C and 1200°C to get larger grain sizes. Following this, they implanted the samples with arsenic and covered the top of the samples with 400 nm of low temperature oxide (LTO). Subsequently, they annealed the samples at temperatures of 800°C and 900°C and measured the diffused chemical profiles using Rutherford backscattering (RBS).

Fig. 2.3 shows the RBS spectra observed by Swaminathan *et al.* for three different starting grain sizes. It can be clearly seen from the figure that the concentration in the tail region of the profile increases with diminishing initial grain size. A smaller grain size means a larger grain boundary volume which leads to more segregation to and diffusion in the grain boundary and hence a higher concentration in the tail region.

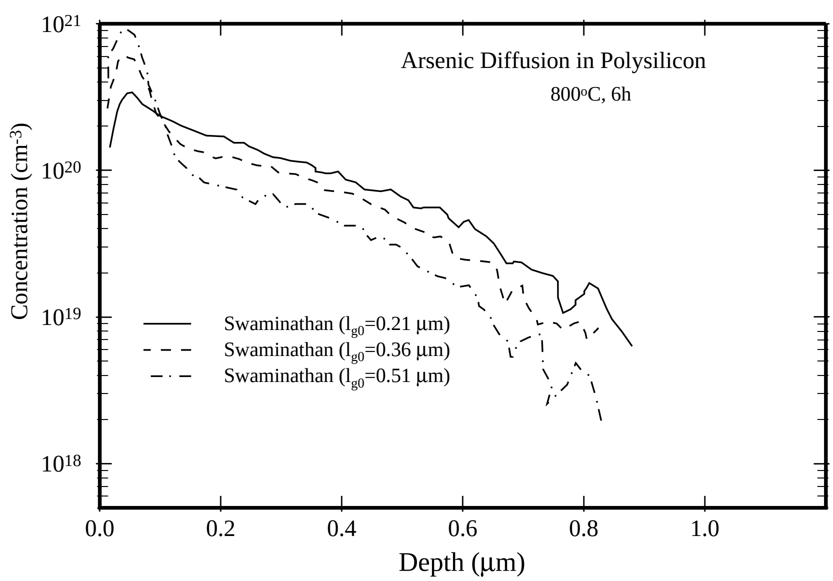

Figure 2.3: RBS data from Swaminathan *et al.* [33] for arsenic diffusion in polysilicon with varying initial grain sizes. Annealed at 800°C for 6h.

As discussed earlier, polysilicon consists of single crystal grains separated by regions of highly disordered grain boundaries. Because of the high defect concentrations within the grain boundaries, dopant diffusivities are increased 100 - 1000 times in the grain boundaries. Thus during annealing, dopants at the grain boundaries diffuse rapidly along the grain boundaries.

The most commonly used model for dopant diffusion in polysilicon (for example in SUPREM IV) simply assumes a higher effective diffusivity, increased by a factor of 100. Although this is sufficient to predict the dopant profiles for high thermal budgets (long anneal times or high temperatures), where the dopant profile within the poly is essentially flat, this cannot do justice to low thermal budget anneals as can be seen in Fig 2.4.

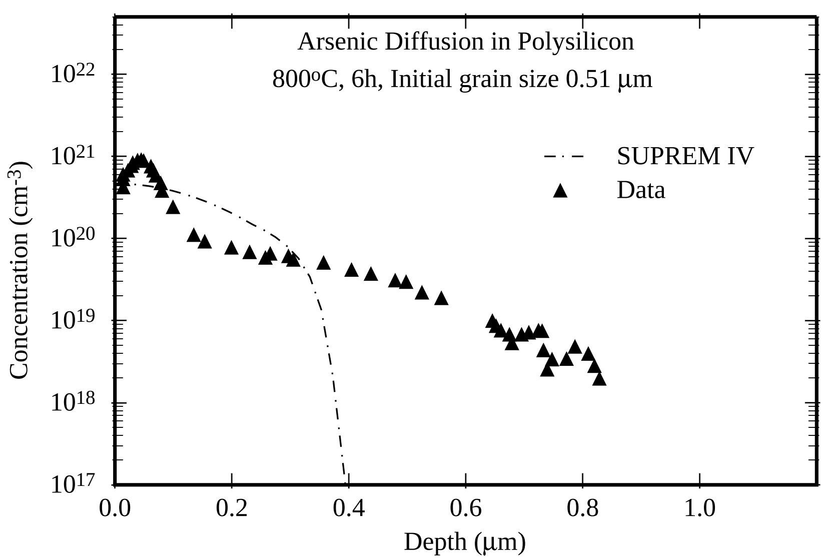

Figure 2.4: Comparison of SUPREM IV simulation to experimental data from Swaminathan *et al.* [33]. Diffusion of arsenic for 6 h at 800°C

Numerous models have been proposed to explain dopant diffusion in polysilicon [29, 35, 36, 37, 38, 39]. A two-stream model appears to be the popular choice, where the total dopant concentration is divided between the grain and the grain boundary, coupled together by dopant transfer from one to the other. Sadovnikov *et al.* have proposed both a 1D as well as a 2D model for boron diffusion in polysilicon [29, 35]. They have considered grain boundary motion, segregation of dopants to the grain boundaries and different diffusivities in the grain and the grain boundaries and have tried to derive an expression for effective dopant diffusivity in silicon with concentrations near solubility limit. They have also accounted for the influence of interfacial oxide layer thickness on polysilicon to silicon diffusion. O'Neill *et al.* [39] have developed a 1D model which is essentially one-stream in nature and neglects the grain interior diffusion and clustering physics. Jones *et al.* [36, 37] have presented a 2D model which considers grain growth fitted to data based on a square root of time dependence and transfer of dopants from grains to grain boundaries based on both diffusion and grain growth. Puchner *et al.* [53] have presented a two-stream model using a static clustering model and a detailed grain growth model. They have calibrated their model on experiments they have carried out themselves.

Chapter 3

The Two Stream Model

As discussed earlier, dopant diffusivities have been observed to be significantly enhanced in polysilicon. Polysilicon microstructure shows single crystal grains separated by areas of high defect concentrations called grain boundaries. As a result, dopants within the grain boundaries have a larger diffusivity and this phenomenon leads to a overall higher diffusivity in polysilicon. However, we have seen that just increasing the average value of single crystal silicon diffusivity for dopants and then treating polysilicon as single crystal material is not sufficient to model dopant diffusion in polysilicon. To be able to predict dopant profiles with significant accuracy under varying conditions, we need to be able to model the fundamental physics going on in polysilicon.

For an efficient model to represent this complex mechanism of dopant diffusion in polysilicon, one has to consider the several transport mechanisms going on. Dopants like arsenic and phosphorus tend to segregate preferentially to the grain boundaries. As a result, there is a diffusive flux of the dopants from the grain interiors to the grain boundaries with a diffusivity as in single crystal silicon. Once the dopants reach the grain boundaries, they segregate to the grain boundaries trying to establish the equilibrium segregation ratio. In addition to this, grains are growing during the high temperature anneal and as the grain boundaries sweep across grains, they pick up dopants. Once the dopants reach the grain boundaries, they diffuse rapidly throughout the polysilicon film. Also, dopants diffuse towards the substrate through the grain interiors. But with the much lower values of diffusivity in the grain interiors, outside the implanted region, the concentrations within the grain boundaries are much higher than in the grain interiors and to maintain an equilibrium segregation ratio, dopants move out of the grain boundaries into the grains. Fig. 3.1 illustrates all these different dopant transport mechanisms.

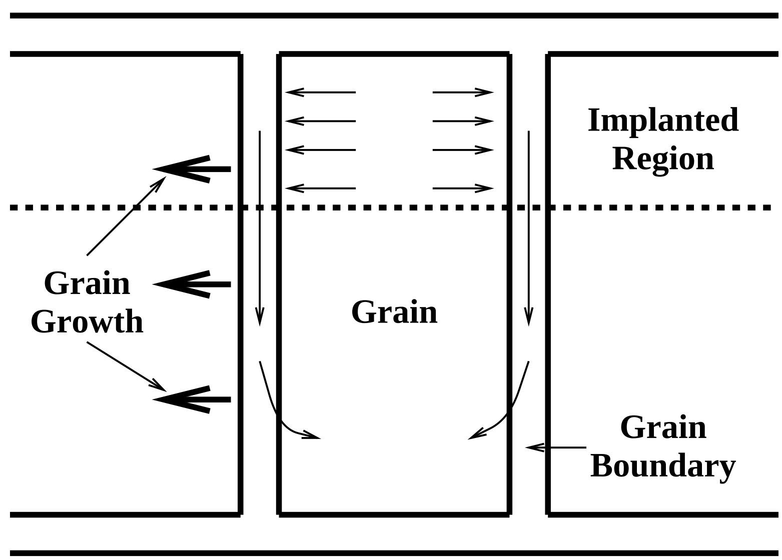

Figure 3.1: Schematic of dopant diffusion mechanisms in polysilicon

Of the two mechanisms of dopant transfer to the grain boundaries, we find grain boundary motion to be the dominant mechanism under most conditions. Grains grow rapidly in the peak region of the implants and thus the grain boundaries pick up dopants as they sweep through the grains. Since the dopant concentration in the tail region of the profile is dominated by the concentration in the grain boundaries, a model not incorporating effects of grain growth grossly underestimates the tail region of the profile as shown in Fig. 3.2.

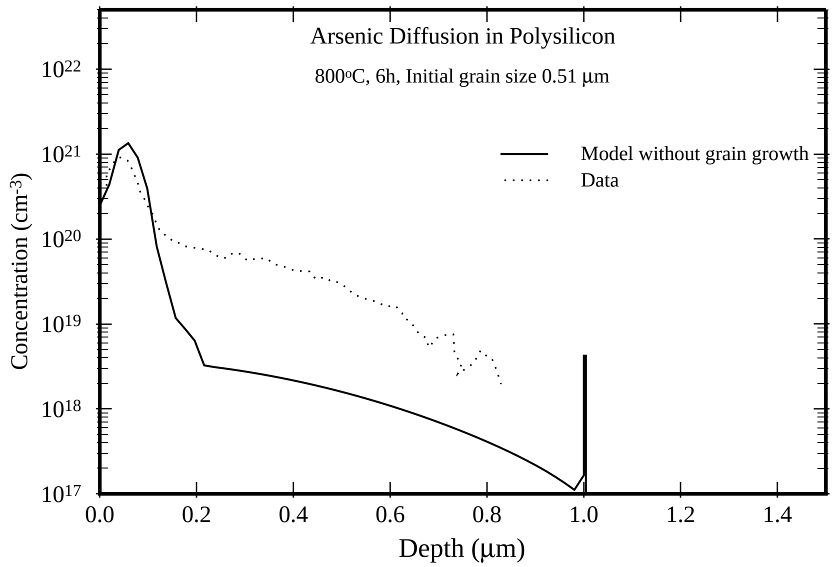

Figure 3.2: Comparison of a static 2D model which does not incorporate grain growth to RBS data from Swaminathan *et al.* [33]. Annealed at 800°C for 6h.

We need to model these various dopant transport mechanisms in polysilicon and also the accompanying microstructural changes in polysilicon. As observed earlier, the grains in polysilicon grow when polysilicon is annealed at the regular processing temperatures. The rate of growth of grains is dependent on temperature as well as dopant concentrations. To incorporate all these effects in addition to the fundamental physics of diffusion in a 2D model is a complicated job. However, effects of grain growth can be incorporated relatively easily in a two stream model [37, 53, 29]. The two stream model divides the total dopant population into the ones that are inside the grain and those that are in the grain boundary regions. The physics of diffusion is different for the grain population and the grain boundary population. The two stream model allows for this to be implemented with the two streams being strongly coupled to one another by various dopant transport mechanisms between the two streams.

The different mechanisms for dopant transport in polysilicon are listed below:

- Dopant diffusion within the polysilicon through the grain interiors.

- Dopant diffusion through the polysilicon along the grain boundaries.
- Dopant transfer from the grain interior regions to the grain boundary regions by diffusive flux from the center of the grains towards the boundaries.
- Dopant transfer into the grain boundaries from the grain interiors due to grain growth
- Dopant segregation to the grain boundaries.

Segregation and grain growth are two very important features of the model we will be discussing here. Each of the two requires extensive study to understand the physics of the processes and we will discuss these two processes before we discuss the full model for dopant diffusion in polysilicon.

3.1 Segregation of Dopants to the Grain Boundaries

Segregation is the process by which dopant atoms move into the grain boundaries from the grain and vice versa. The main driving force behind this being the fact that the system can lower its energy by moving dopant atoms into the grain boundaries. There is an equilibrium ratio between the atoms that are in the grain interiors and the ones in the grain boundaries. However, there are only a fixed number of sites in the grain and the grain boundaries that the dopant atoms can occupy.

Let $C_{\mathrm{A}}^{\mathrm{g}}$ be defined as the concentration of dopant A in the grain interior averaged over both the grain and the grain boundary volumes i.e.

$$C_{\mathrm{A}}^{\mathrm{g}} = \left(\frac{\text{number of dopants in grain interior}}{\text{unit polysilicon volume}}\right) \tag{3.1}$$

and $C_{\mathrm{A}}^{\mathrm{gb}}$ is defined as the concentration of dopant A in the grain boundary averaged over both the grain and grain boundary volumes i.e

$$C_{\mathrm{A}}^{\mathrm{gb}} = \left(\frac{\text{number of dopants in grain boundary}}{\text{unit polysilicon volume}}\right) \tag{3.2}$$

By defining the two concentrations in this way, it is possible to get the total concentration in polysilicon as the sum of the individual concentrations in the grain and the grain boundary. Thus,

$$C_{\mathrm{total}} = C_{\mathrm{A}}^{\mathrm{g}} + C_{\mathrm{A}}^{\mathrm{gb}}. \tag{3.3}$$

Also, we define Q_{gb} as the number of grain boundary sites per unit area that the dopant atoms could occupy. X_{gb} is defined to be the fraction of grain boundary sites occupied by the dopants and X_{g} as the fraction of grain sites occupied by the dopants. Hence, we have

$$X_{\mathrm{g}} = \frac{C_{\mathrm{A}}^{\mathrm{g}}}{N_{\mathrm{Si}}}, \tag{3.4}$$

where we assume that the grain interior is identical to single crystal silicon and the grain boundary volume is negligible compared to that of the grains and

$$X_{\mathrm{gb}} = \frac{C_{\mathrm{A}}^{\mathrm{gb}}\, L_{\mathrm{g}}}{2\, Q_{\mathrm{gb}}}, \tag{3.5}$$

with the $L_{\mathrm{g}}/2$ factor coming in because we defined $C_{\mathrm{A}}^{\mathrm{gb}}$ to be defined over unit polysilicon volume instead of just grain boundary volume.

Th rate at which dopants are moving out from the grains to the grain boundaries is proportional to the fraction of filled sites in the grain and to the fraction of empty sites in the grain boundaries. Likewise, the rate at which dopants are moving out from the grain boundaries into the grain is proportional to the fraction of filled sites in the grain boundaries and the fraction of empty sites in the grains. At equilibrium these two rates must be equal with an equilibrium constant which depends on the reduction in energy ($\triangle\, G_s$) associated with dopants moving into grain boundary sites.

Therefore in equilibrium, we get,

$$m\, X_{\mathrm{g}}\,(1\,-\,X_{\mathrm{gb}})\;=\;X_{\mathrm{gb}}\,(1\,-\,X_{\mathrm{g}}), \tag{3.6}$$

where m is the equilibrium segregation coefficient and is of the form

$$m\;=\;\exp\left(\frac{\triangle G_s}{k\,T}\right)\;=\;m_0\,\exp\left(\frac{\triangle\,H_s}{k\,T}\right) \tag{3.7}$$

with $\triangle H_s$ the enthalpy change associated with the process.

We can safely assume that $X_{\mathrm{g}}\,\ll\,1$, since the grain interiors have a huge number of sites to incorporate the dopants. Hence we can rewrite Eq. 3.6 as

$$X_{\mathrm{g}}\;=\;\frac{X_{\mathrm{gb}}}{m\,(1\,-\,X_{\mathrm{gb}})} \tag{3.8}$$

Substituting for X_{g} and X_{gb}, we get,

$$\frac{C_{\mathrm{A}}^{\mathrm{g}}}{N_{\mathrm{Si}}}\;=\;\frac{C_{\mathrm{A}}^{\mathrm{gb}}\left(\frac{L_{\mathrm{g}}}{2\,Q_{\mathrm{gb}}}\right)}{m\,\left[1-\left(\frac{C_{\mathrm{A}}^{\mathrm{gb}}\,L_{\mathrm{g}}}{2\,Q_{\mathrm{gb}}}\right)\right]} \tag{3.9}$$

On rearranging we get,

$$\frac{C_{\mathrm{A}}^{\mathrm{gb}}}{C_{\mathrm{A}}^{\mathrm{g}}}\;=\;\left(\frac{2\,m\,Q_{\mathrm{gb}}}{N_{\mathrm{Si}}\,L_{\mathrm{g}}}\right)\,\left(1-\frac{C_{\mathrm{A}}^{\mathrm{gb}}\,L_{\mathrm{g}}}{2\,Q_{\mathrm{gb}}}\right) \tag{3.10}$$

which gives us

$$s\;=\;\frac{C_{\mathrm{A}}^{\mathrm{gb}}}{C_{\mathrm{A}}^{\mathrm{g}}}\;=\;\frac{2\,m\,Q_{\mathrm{gb}}}{N_{\mathrm{Si}}\,L_{\mathrm{g}}\,\left(1+\frac{m\,C_{\mathrm{A}}^{\mathrm{g}}}{N_{\mathrm{Si}}}\right)} \tag{3.11}$$

where s is the effective segregation coefficient between the grain and the grain boundary, giving the equilibrium ratio between the concentrations in the grain and the grain boundary averaged over both grain and grain boundary volumes.

We have characterized this model for segregation based on experimental data from

Mandurah *et al.* [26] and Demirlioglu [28] and the results will be presented in Chapter 5.

3.2 Grain Growth

Grain growth is an important phenomenon in most polycrystalline materials. The rate of growth has been found to be proportional to t^n where $0 < n < 1$. For grain growth in polysilicon, we use a model similar to that developed by Kim and Thompson [11] where

$$\frac{\partial L_{\mathrm{g}}}{\partial t} = \frac{\sigma}{L_{\mathrm{g}}} \tag{3.12}$$

so that

$$L_{\mathrm{g}}^2 = L_{\mathrm{g}0}^2 + 2\,\sigma\,t. \tag{3.13}$$

Assuming that grain growth occurs due to grain boundary migration through either dislocation glide or climb and that these processes are additive, the grain boundary mobility can be expressed as

$$M = M_1 + M_2 \tag{3.14}$$

where M_1 represents the glide component and M_2 represents the climb component. Also, we assume that the climb or diffusive component is related to the total vacancy concentration, giving

$$M_2 = K\,C_V \tag{3.15}$$

where K is a temperature dependent constant and C_V is the total vacancy concentration.

The vacancy concentration is dependent on the Fermi level and therefore the dopant concentration as well as temperature. Assuming that the non-diffusive component M_1 is not affected by the dopant concentration, we can write based on Eqs.

3.14 and 3.15,

$$M \;=\; M_1 \left[1 \,+\, K^{'} \left(\frac{C_V^e}{C_V^i}\right)\right]. \tag{3.16}$$

Kim and Thompson [11] report values of $K^{'}$ as $2.5 \times 10^4 \exp\left(-1.1\, eV/kT\right)$ based on their experiments. From Eq. 2.4 we can write down σ as

$$\sigma \;=\; \alpha\, \gamma_{\mathrm{gb}}\, M_1 \left[1 \,+\, K^{'} \left(\frac{C_V^e}{C_V^i}\right)\right] \tag{3.17}$$

It has been observed by Kim and Thompson [11] that primary grain growth stops when the grain size becomes about 4 times the film thickness. To account for this behavior, we modify σ derived in Eq. 3.17 as

$$\sigma \;=\; \alpha\, \gamma_{\mathrm{gb}}\, M_1 \left[1 \,+\, K^{'} \left(\frac{C_V^e}{C_V^i}\right)\right] \left(1 \,-\, \frac{L_{\mathrm{g}}}{4\, t_f}\right) \tag{3.18}$$

where t_f is the film thickness.

Angelucci *et al.* [17] and Mei *et al.* [13] have observed that at concentrations above solid solubility, increasing arsenic concentration significantly reduces grain growth whereas phosphorus doping results in continued increase. Below solid solubility, increases in grain growth are well-modeled by changes in vacancy concentration, increasing strongly with doping. Thus in contrast to metals [40], solute drag (a reduction in grain growth due to high solute concentrations) does not seem to be significant. Instead, we assume (as suggested by Angelucci *et al.* [17]) that the formation of arsenic precipitates near the grain boundary slows down grain boundary mobility. Thus, we further modify σ derived in Eq. 3.18 as

$$\sigma \;=\; \alpha\, \gamma_{\mathrm{gb}}\, M_1 \left[1 \,+\, K^{'} \left(\frac{C_V^e}{C_V^i}\right)\right] \left(1 \,-\, \frac{L_{\mathrm{g}}}{4\, t_f}\right) \left(\frac{1}{1 \,+\, \dfrac{C_{\mathrm{g}}^{\mathrm{tot}} \,-\, C_{\mathrm{g}}^{\mathrm{act}}}{C_{\mathrm{r}}}}\right) \tag{3.19}$$

where $C_{\mathrm{g}}^{\mathrm{tot}} \,=\, C_{\mathrm{A}}^{\mathrm{gb}}/s$ is the total concentration of dopants near the grain boundary and $C_{\mathrm{g}}^{\mathrm{act}} = \min(C_{\mathrm{A}}^{\mathrm{gb}}/s, C^{\mathrm{ss}})$ is the active concentration near the grain boundaries. C_{r} is an empirical parameter whose value has been determined from experimental data from Angelucci *et al.* [17].

3.3 Rate of Transfer of Dopants From Grain to Grain Boundaries

The two dopant concentrations $C_{\mathrm{A}}^{\mathrm{g}}$ and $C_{\mathrm{A}}^{\mathrm{gb}}$ are coupled together by transfer of dopants from the grains to the grain boundaries. When the system is in equilibrium, there would be no net dopant transfer from the grains to the grain boundaries and we would have

$$C_{\mathrm{A}}^{\mathrm{g}} = \frac{C_{\mathrm{A}}^{\mathrm{gb}}}{s}. \tag{3.20}$$

However, when the system is not in equilibrium, the dopant transfer is proportional to the difference from the equilibrium values and we call the rate of transfer k_{eff}.

There are two processes that lead to dopant transfer from the grains to the grain boundaries. Due to segregation of dopants from the grains to the grain boundaries, the region of the grains near the grain boundaries gets depleted of dopants. As a result, a concentration gradient is built up between the center of the grains and the grain edges. This leads to a diffusion flux of dopants from the center of grains towards the grain boundaries and the transfer rate arising out of this is termed k_D. At the same time, as the grains grow, the grain boundaries sweep through the polysilicon picking up (or leaving behind) dopants as they move. The rate at which dopants are transferred as a result of grain boundary movement is defined as k_V. We can approximate the net effective transfer rate as the sum of these two effects,

$$k_{\mathrm{eff}} = k_D + k_V. \tag{3.21}$$

3.3.1 Estimation of k_D

As the dopant segregates from the grains to the grain boundaries, the dopant concentration near the grain boundary drops and we get a variation in concentration within the grain. As a result there is a dopant flux from the center of the grains towards the boundaries. Let us assume a grain of diameter L_{g} which is not growing in time with the center of the grain at $x = 0$. The diffusion equation for the excess concentration C (C is defined as concentration within the grain minus the concentration near the grain boundaries) inside the grain in 1D is

$$\frac{\partial C}{\partial t} = D_{\mathrm{A}}^{\mathrm{g}} \frac{\partial^2 C}{\partial x^2}, \tag{3.22}$$

with the initial condition being

$$C(x, t = 0) = C_0 \tag{3.23}$$

and the boundary conditions being

$$C(x = -L_{\mathrm{g}}/2, t) = C(x = L_{\mathrm{g}}/2, t) = 0 \tag{3.24}$$

On solving this system, we get

$$C(x,t) = C_0 - C_0 \sum_{n=0}^{\infty} \left[(-1)^n \left(\mathrm{erfc} \left(\frac{(n+1/2)L_{\mathrm{g}} - x}{2\sqrt{D\,t}} \right) + \mathrm{erfc} \left(\frac{(n+1/2)L_{\mathrm{g}} + x}{2\sqrt{D\,t}} \right) \right) \right] \tag{3.25}$$

However, we can see from Fig. 3.3 that $C(x,t)$ can be well represented by just taking the first term in the sum of complementary error functions and we can write

$$C(x,t) = C_0 \left[1 - \mathrm{erfc} \left(\frac{L_{\mathrm{g}}/2 - x}{2\sqrt{D\,t}} \right) - \mathrm{erfc} \left(\frac{L_{\mathrm{g}}/2 + x}{2\sqrt{D\,t}} \right) \right]. \tag{3.26}$$

We can define the diffusive transfer rate as the ratio of the flux at the boundary to the total excess doping in the grain which gives us

$$k_D = \frac{D \dfrac{\partial C}{\partial x} \mid_{x=L_g/2}}{\displaystyle\int_0^{L_g/2} C\, dx} \tag{3.27}$$

We should note that this analysis is valid for 1D grains and to extend it to cylindrical grains we need to multiply the k_D value obtained in the equation above by a factor of 2 since the ratio of area to volume is 2 times larger. Hence k_D becomes

$$k_D = \frac{4\sqrt{D_{\mathrm{A}}^{\mathrm{g}}}\left[1 - \exp\left(\dfrac{-L_{\mathrm{g}}^2}{4\, D_{\mathrm{A}}^{\mathrm{g}}\, t}\right)\right]}{\sqrt{\pi\, t}\left[L_{\mathrm{g}} - 2\, L_{\mathrm{g}}\, \mathrm{erfc}\left(\dfrac{L_{\mathrm{g}}}{2\sqrt{D_{\mathrm{A}}^{\mathrm{g}}\, t}}\right) + 4\sqrt{\dfrac{D_{\mathrm{A}}^{\mathrm{g}}\, t}{\pi}}\left(1 - \exp\left(\dfrac{-L_{\mathrm{g}}^2}{4\, D_{\mathrm{A}}^{\mathrm{g}}\, t}\right)\right)\right]} \tag{3.28}$$

If we assume that $\sqrt{D_{\mathrm{A}}^{\mathrm{g}}\, t} \ll L_{\mathrm{g}}$, we can further simplify the above estimate for k_D to

$$k_D = \frac{4}{\sqrt{\pi} L_{\mathrm{g}}}\left(\frac{D_{\mathrm{A}}^{\mathrm{g}}}{\sqrt{D_{\mathrm{A}}^{\mathrm{g}}\, t}}\right). \tag{3.29}$$

Fig. 3.4 shows the comparison of the analytically computed values for k_D with values computed based on the numerical solution of the diffusion equation inside the grain. Sadovnikov *et al.* [35] also carried out analysis based on similar lines, but they missed out a factor of $8/\sqrt{\pi}$ which accounts for their consistent underestimation of the value of k_D. This figure shows that the first term in the analytical solution of $C(x,t)$ is sufficient to estimate the diffusive transfer rate correctly. Fig. 3.4 shows that Eq. 3.29 provides a good approximation to Eq. 3.28 especially at short times. k_D is more important at short times since at long times the concentrations in the grain and the grain boundary are already equlibrated. Hence, we use the much simpler form for k_D described by Eq. 3.29 in our model.

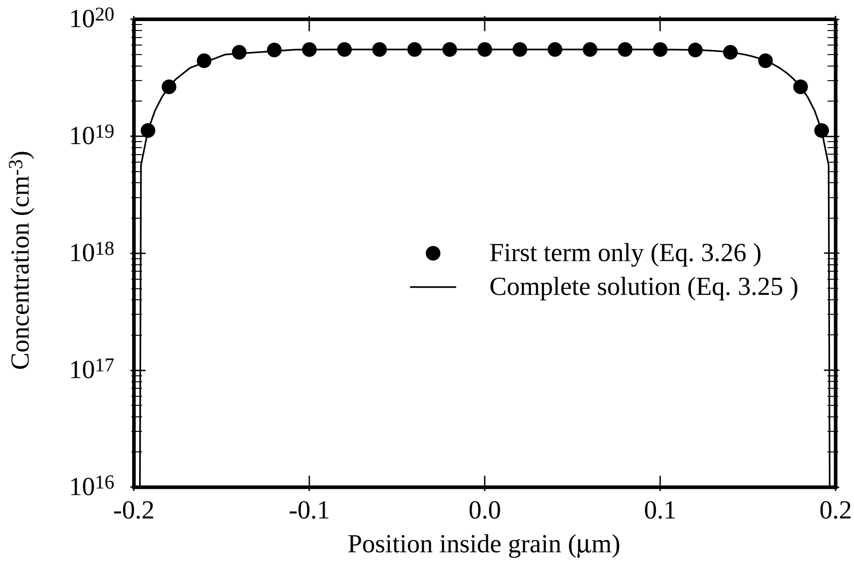

Figure 3.3: $C(x,t)$ plotted as a function of position in the grain after 100 min. anneal at 900°C. This shows that just taking the first term in the summation of the complementary error function is sufficient to approximate the solution.

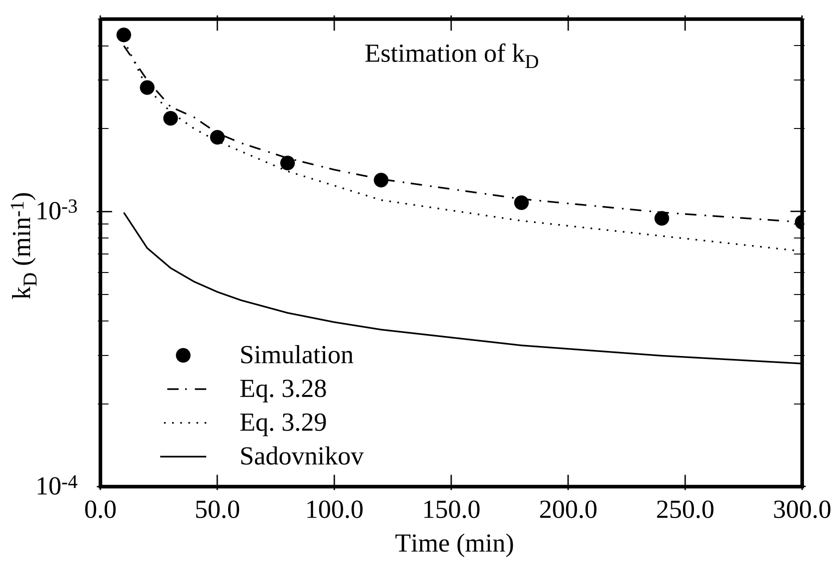

Figure 3.4: Comparison of analytical estimate for value of k_D at 900°C with estimates based on the numerical solution of the diffusion equations inside the grain.

3.3.2 Estimation of k_V

The rate at which grain boundaries pick up dopants is proportional to the rate at which the grains are sweeping out volume. We will do the calculation assuming circular cylindrical grains, although square cylindrical grains give the same result.

Let's assume that the initial size of grains (diameter) is L_1 and the size after a time $\triangle t$ is L_2. Let the film area under consideration be A. Therefore total volume swept out is

$$\begin{aligned}
\triangle V &= \text{decrease in number of grains} \times \text{initial grain size} \qquad (3.30) \\
&= \left(\frac{4\,A}{\pi\,L_1^2} - \frac{4\,A}{\pi\,L_2^2}\right)\frac{\pi\,L_1^2}{4}\,h \\
&= A\,h\left[1 - \left(\frac{L_1}{L_2}\right)^2\right]
\end{aligned}$$

where h is the thickness of the film. Assuming $L_2 = L_1 + \triangle L$, we can write

$$\begin{aligned}
\triangle V &= A\,h\left[1 - \left(\frac{L_1}{L_2}\right)^2\right] \\
&= A\,h\left[1 - \frac{L_1^2}{L_1^2 + 2\,L_1 \triangle L}\right] \\
&= A\,h\left[1 - \frac{1}{1 + (2/L_1)\triangle L}\right] \\
&= A\,h\left[\frac{2}{L_1}\triangle L\right]
\end{aligned}$$

Now, dividing both sides of the above equation by $A\,h$ (the film volume) we get the rate of change of volume per unit volume as

$$\frac{1}{A\,h}\frac{dV}{dt} = \frac{2}{L_1}\frac{dL}{dt}. \qquad (3.31)$$

Since the rate of dopant transfer due to grain boundary movement k_V is the rate of sweeping out of volume by grains per unit volume, we have

$$k_V = \frac{2}{L_\mathrm{g}} \frac{dL_\mathrm{g}}{dt} \tag{3.32}$$

Jones *et al.* [37] use a similar expression for k_V except that they have an empirical factor α multiplying k_V which is chosen to match experimental data.

3.4 The Model Equations

Now that we have analyzed the transport mechanisms in polysilicon, we can write down our continuity equations for the two dopant populations C_A^g and C_A^gb,

$$\frac{\partial C_\mathrm{A}^\mathrm{g}}{\partial t} = \frac{\partial}{\partial x}\left(D_\mathrm{A}^\mathrm{g} \frac{\partial C_\mathrm{A}^\mathrm{g}}{\partial x}\right) - k_\mathrm{eff}\left(C_\mathrm{A}^\mathrm{g} - \frac{C_\mathrm{A}^\mathrm{gb}}{s}\right) \tag{3.33}$$

$$\frac{\partial C_\mathrm{A}^\mathrm{gb}}{\partial t} = \frac{\partial}{\partial x}\left(\frac{D_\mathrm{A}^\mathrm{gb}}{L_\mathrm{g}} \frac{\partial \left(C_\mathrm{A}^\mathrm{gb} L_\mathrm{g}\right)}{\partial x}\right) + k_\mathrm{eff}\left(C_\mathrm{A}^\mathrm{g} - \frac{C_\mathrm{A}^\mathrm{gb}}{s}\right). \tag{3.34}$$

The equations have standard flux terms and are coupled together by the transfer of dopants from the grain to the grain boundaries or vice versa, the rate of this transfer k_eff being the sum of k_D and k_V.

We have defined C_A^gb as the concentration in the grain boundary per unit polysilicon volume, whereas the actual concentration in the grain boundary is per unit grain boundary volume. The driving force for diffusion being the gradient in the actual grain boundary concentration brings the L_g in the numerator in Eq. 3.34. The flux of dopants in the grain boundary is proportional to the grain boundary volume and this explains the L_g in the denominator in Eq. 3.34.

The diffusivity in the grain has been modeled on the lines of the default SUPREM IV model. Values for D_0^g and D_-^g are taken from SUPREM IV default values. The high concentration diffusivity is modeled on the lines of Dunham and Wu [41] and the value for C_{ref} is taken from their work.

$$D_{\text{A}}^{\text{g}} = D_{0}^{\text{g}} + D_{-}^{\text{g}} \left(\frac{n}{n_i}\right) \left[1 + \left(\frac{n}{C_{\text{ref}}}\right)^{3.0}\right] \tag{3.35}$$

For the diffusivity in the grain boundary we use a concentration dependent form as well, since the box shape of the tail region of the dopant profiles suggests such a dependence.

$$D_{\text{A}}^{\text{gb}} = D_{0}^{\text{gb}} + D_{-}^{\text{gb}} \left(\frac{n}{n_i}\right). \tag{3.36}$$

where D_0^{gb} and D_-^{gb} have been chosen to match experimental data.

Chapter 4

Experimental Procedures and Analysis Techniques

4.1 Wafer Processing

The starting material for the experiments was n-type 4-inch Czochralski $\langle 100 \rangle$ silicon wafers with resistivity between 8 and 20 Ω-cm. After a standard RCA clean of the wafers, 1000 Å of silicon dioxide was thermally grown on these wafers by wet oxidation at 1000°C. This was necessary to prevent epitaxial realignment of the polysilicon that was deposited on top of the silicon substrate. It has been observed that when polysilicon is deposited on a single crystal silicon substrate, during high temperature annealing steps the native oxide between the polysilicon and monosilicon breaks down. As a result, the polysilicon layer on top starts to realign to the single crystal substrate and loses its polycrystalline nature.

8000 Å of polysilicon was deposited on top of the oxide by LPCVD at 625°C at a pressure of 200 mTorr. SEM and TEM measurements (explained later on) were carried out to measure the average grain size in polysilicon after deposition. This was found to be approximately 0.2 μm. This is referred to as the as-deposited grain size. Since we wanted to investigate the effects of initial grain size (i.e. grain size at

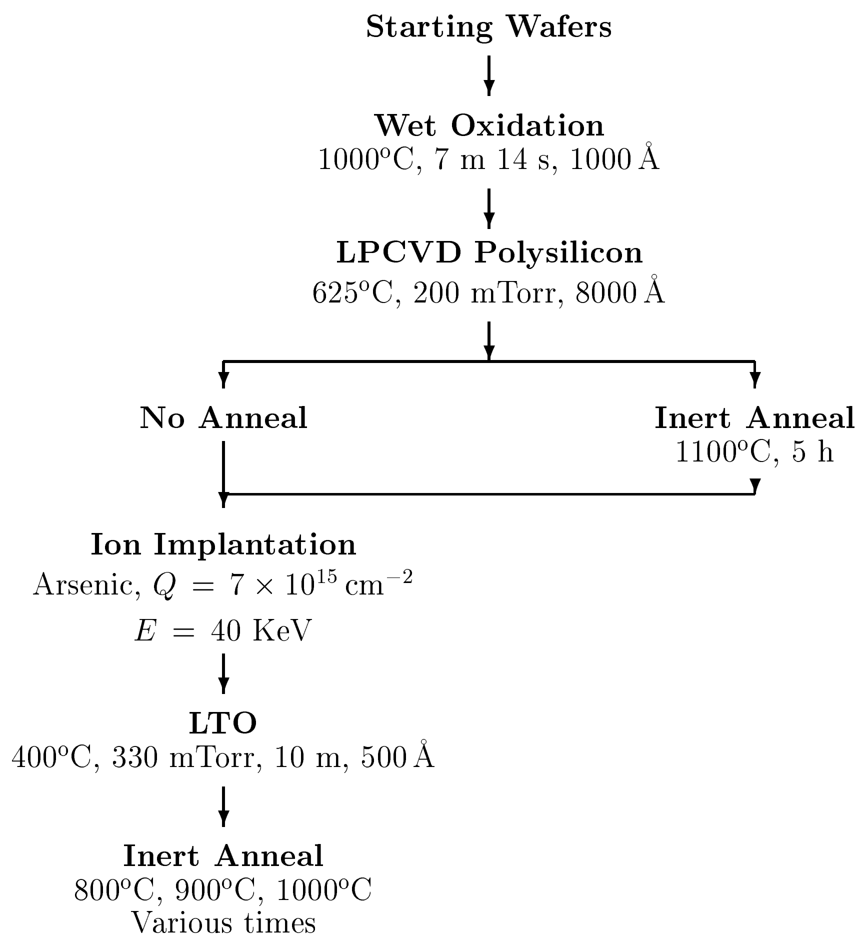

Figure 4.1: Wafer processing steps

the beginning of the anneal process), we annealed some of the samples at 1100°C for a time of 5 h. This led to grain growth and thus a larger initial grain size of about 0.25 μm. Following this, arsenic was implanted into polysilicon at an energy of 40 keV and a dose of $7 \times 10^{15}\,\mathrm{cm}^{-2}$. A low temperature oxide (LTO) was then deposited on the polysilicon as a cap to prevent out diffusion of arsenic during subsequent high temperature annealing. The thickness of the LTO was 500 Å and was deposited at 400°C.

The samples were annealed in a nitrogen ambient for different lengths of time at different temperatures to investigate the effect of temperature on dopant diffusion in polysilicon. Furnace anneals were carried out at temperatures of 800°C and 900°C, whereas rapid thermal anneals were used at 1000°C.

At 800°C, samples were annealed for 5 h. However, due to the mechanical system of loading the wafers in the furnace, there was an additional time of 6 min for the wafers to be pushed in, 10 min for stabilization of furnace temperature and 6 min for the wafers to be pulled out of the furnace. A control wafer was put through this cycle of being pushed into the furnace, stabilization and being pulled out of the furnace to see how much diffusion occurred. This sample also provided insight into how much transient enhanced diffusion (TED) occurred and whether any dopant redistribution or segregation to grain boundaries occurred during epitaxial regrowth of the polysilicon layer that was amorphized during the arsenic implant.

At 900°C, samples were annealed for times of 15 min, 30 min and 1 h. In addition to the anneal time, the samples also underwent a 6 min boat-in, 10 min of stabilization at 800°C, 8 min ramp up to 900°C, 15 min of ramp down to 800°C and a final 6 min of boat-out. As for the 800°C anneal, a control wafer was processed through this cycle.

At 1000°C, RTA was carried out on the samples for times of 5 s and 15 s. Since, the ramp up and ramp down time in a RTA system is negligible, we did not use a control wafer in this case.

4.2 Analysis Techniques

Grain size measurements were carried out by SEM and TEM. SEM photographs show that the surface of polysilicon has grains which are roughly circular in cross-section. However, the resolution of the SEM equipment was not high enough to clearly distinguish the boundaries of each grain. As a result, grain size measurements based on SEM photographs are subject to relatively large errors. To enhance the contrast between the grains and the grain boundaries, the samples were etched in a solution comprising of nitric acid, water and hydrofluoric acid in the ratio 55:16.7:1. This etchant etches polysilicon with different etch rates in the grains and the grain boundaries. As a result, the contrast was expected to be better. We etched samples for a time of 4 s. Longer etch times made the material look amorphous without any grains being visible. Figs. 4.2 and 4.3 show a comparison of SEM pictures after an etch of 3 s and 10 s respectively. Based on all SEM measurements we estimated the as-deposited grain size to be 0.2 μm. SEM measurements were carried out on a sample after it went through the 900°C, 1 h anneal which showed a final grain size of approximately 0.32 μm.

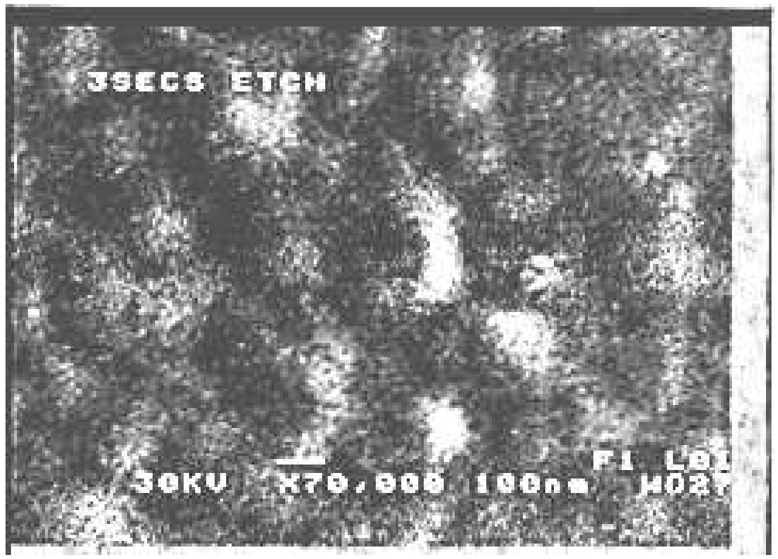

Figure 4.2: SEM picture of as-deposited polysilicon after 3 s etch for grain boundary delineation.

To get a more accurate estimate of the as-deposited grain size, we carried out TEM on some of the samples. The contrast is excellent with plan view TEM and grains can be clearly seen. Measurements carried out on samples showed that the as-deposited grain size in polysilicon is 0.2 μm corroborating the SEM measurement.

Dopant profiles were measured by secondary ion mass spectroscopy (SIMS) carried out at Evans East in New Jersey. Fig. 4.4 shows an example of an arsenic profile after implant and after an additional 5 h anneal at 800°C.

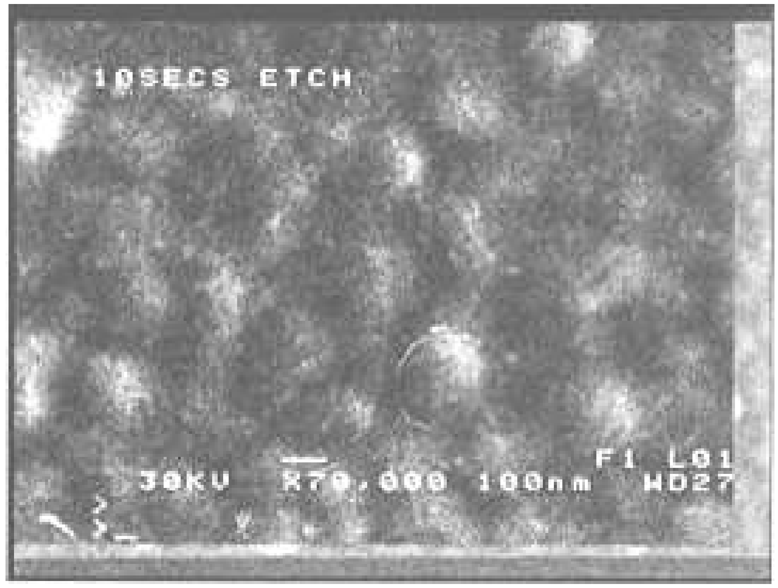

Figure 4.3: SEM picture of as-deposited polysilicon after 10 s etch for grain boundary delineation.

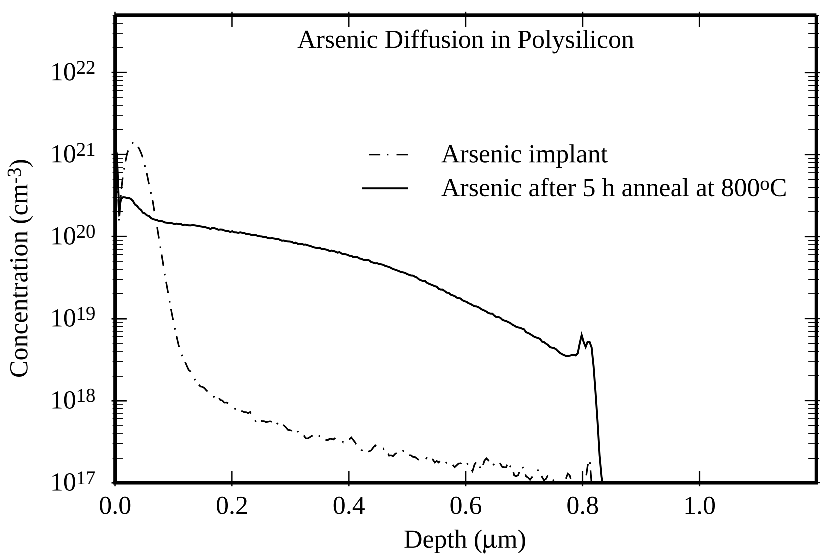

Figure 4.4: SIMS profiles for the As implant and after a 800°C, 5 h anneal.

Chapter 5

Results and Discussion

In this chapter, the models for dopant segregation and grain growth described in Chapter 3 are characterized based on experimental results. These parameters are then used in the two-stream polysilicon diffusion model and the resulting predicted dopant profiles are compared with experiments.

5.1 Segregation

As discussed Section 3.1, dopants (especially arsenic and phosphorus) in polysilicon have a tendency to segregate preferentially to the grain boundaries with an equilibrium segregation ratio defined by

$$s = \frac{C_{\mathrm{A}}^{\mathrm{gb}}}{C_{\mathrm{A}}^{\mathrm{g}}} = \frac{2\, C_{\mathrm{A}}^{\mathrm{g}}\, m\, Q_{\mathrm{gb}}}{N_{\mathrm{Si}}\, L_{\mathrm{g}} \left(1 + \dfrac{m\, C_{\mathrm{A}}^{\mathrm{g}}}{N_{\mathrm{Si}}}\right)}. \tag{5.1}$$

Looking at this relationship we notice that the effective equilibrium segregation ratio decreases with increasing grain size, as well as with increasing grain concentration and increasing temperature. As a result, to calculate the segregation parameters from experimental results, it is critical to know the grain size at the time when the grain and the grain boundary concentrations are measured. The grain concentration was measured using Hall measurements which gives the active concentration. Assuming that the dopants in the grain boundary are inactive, the grain boundary concentration is the difference between the total concentration and the active concentration. Mandurah *et al.* [26] carried out segregation experiments assuming that after their initial 1000°C anneal for 1 h, the implanted dopants were uniformly distributed in polysilicon and that the grain sizes were stabilized. However, we simulated the same low temperature long time anneals and concluded that significant grain growth can be expected during this time. This has also been observed in similar experiments by Demirlioglu [28]. Hence, by using the grain size after the initial 1000°C anneal for calculating the equilibrium segregation ratio at lower temperatures, they overestimated this ratio. To correct for this error, we carried out the same calculations, but used the increased grain size based on simulations of grain growth. Based on data by Mandurah *et al.* at different temperatures for various dopant concentrations, we fitted our expression for s to match this data. Since Eq. 5.1 can be rewritten as

$$C_{\mathrm{A}}^{\mathrm{gb}}\,L_{\mathrm{g}} = \frac{2\,C_{\mathrm{A}}^{\mathrm{g}}\,m\,Q_{\mathrm{gb}}}{N_{\mathrm{Si}}\left(1+\dfrac{m\,C_{\mathrm{A}}^{\mathrm{g}}}{N_{\mathrm{Si}}}\right)}, \tag{5.2}$$

we plot $C_{\mathrm{A}}^{\mathrm{gb}}\,L_{\mathrm{g}}$ vs. $C_{\mathrm{A}}^{\mathrm{g}}$ for the data from Mandurah *et al.* in Fig. 5.1.

This figure also illustrates the effect of incorporating saturation of grain boundary sites. Assuming that there is only a fixed number of sites in the grain boundary to which the dopant atoms can segregate to, we expect that the grain boundary concentration will not increase linearly with grain concentration. This is reflected in the data as well as in the model as can be seen for the 800°C case in Fig. 5.1. The estimated value of Q_{gb} for arsenic turns out to be 2.1×10^{15} cm^{-2} which is a reasonable estimate based on first principle calculations of the number of dangling bonds in the grain boundaries by [57].

Demirlioglu [28] carried out similar experiments for phosphorus but taking into account grain growth during the low temperature anneals. Fig. 5.2 shows a compar-

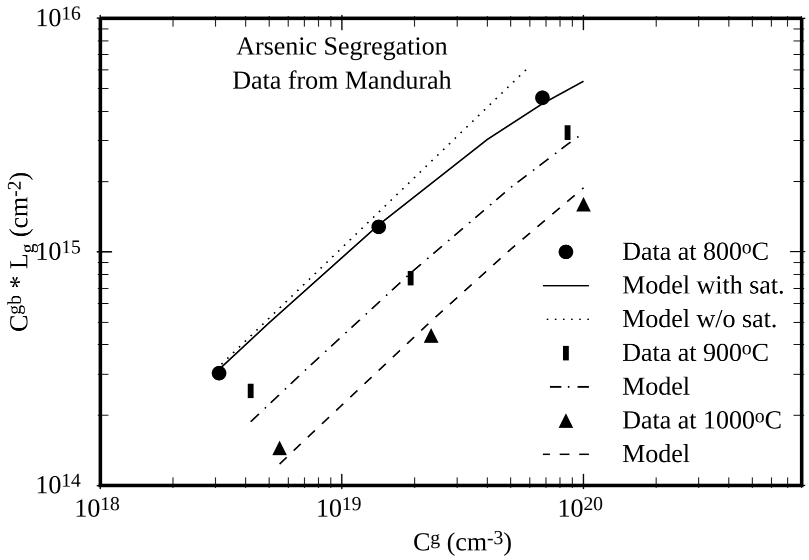

Figure 5.1: Comparison of model to experimental data for $C_{\mathrm{A}}^{\mathrm{gb}}\,L_{\mathrm{g}}$ vs $C_{\mathrm{A}}^{\mathrm{g}}$ as reported by Mandurah *et al.* For the lowest temperature, the effect of including saturation of grain boundary sites in the model is also shown.

ison of data from her experiments with the model predictions. Table 5.1 below lists the segregation parameter values for arsenic and phosphorus, where

$$m = m_0 \exp\left(\frac{-\triangle H_s}{k\,T}\right). \tag{5.3}$$

	m_0	$\triangle H_s$ (eV)	Q_{gb} (cm^{-2})
Arsenic	0.081	0.81	2.1×10^{15}
Phosphorus	0.028	0.90	5.6×10^{15}

Table 5.1: Segregation parameter values for arsenic and phosphorus.

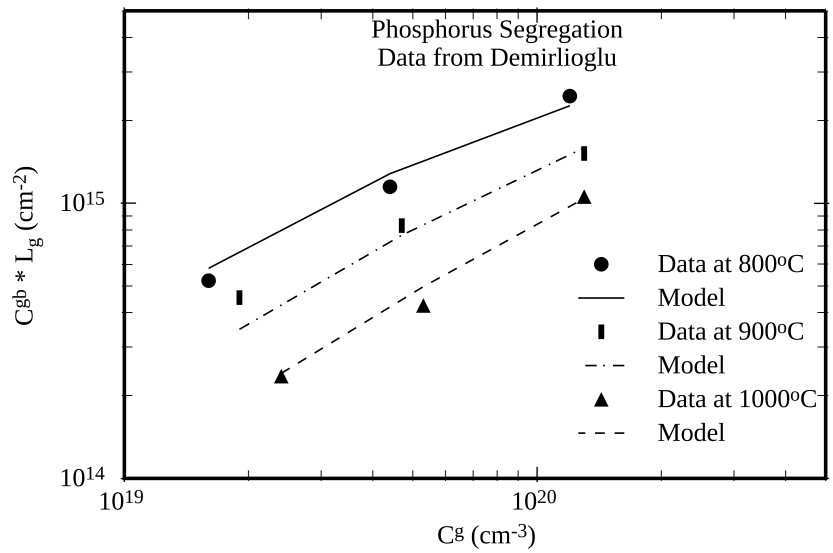

Figure 5.2: Comparison of model to experimental data for $C_{\mathrm{A}}^{\mathrm{gb}}\, L_{\mathrm{g}}$ vs $C_{\mathrm{A}}^{\mathrm{g}}$ as reported by Demirlioglu.

5.2 Grain Growth

Grain growth has been modeled with a square root of time dependence as discussed in Section 3.2.

$$\frac{\partial L_{\mathrm{g}}}{\partial t} = \frac{\sigma}{L_{\mathrm{g}}} \tag{5.4}$$

and

$$\sigma = \alpha\, \gamma_{\mathrm{gb}}\, M_1 \left[1 + K' \left(\frac{C_V^e}{C_V^i}\right)\right] \left(1 - \frac{L_{\mathrm{g}}}{4\, t_f}\right) \left(\frac{1}{1 + \dfrac{C_{\mathrm{g}}^{\mathrm{tot}} - C_{\mathrm{g}}^{\mathrm{act}}}{C_{\mathrm{r}}}}\right). \tag{5.5}$$

Values for K' have been taken from Kim and Thompson [11] and $\alpha\, \gamma_{\mathrm{gb}}\, M_1$ has been optimized to match experimental grain growth data from Wada *et al.* [16]. Fig. 5.3 shows the grain sizes obtained for an anneal of 1 h at temperatures ranging from 800°C to 900°C when the total dopant concentration in the polysilicon is 7.5×10^{20} cm^{-3}. Fig. 5.4 shows comparison of model with experimental data (Wada *et al.* [16])

of grain growth vs. anneal time for two different anneal temperatures.

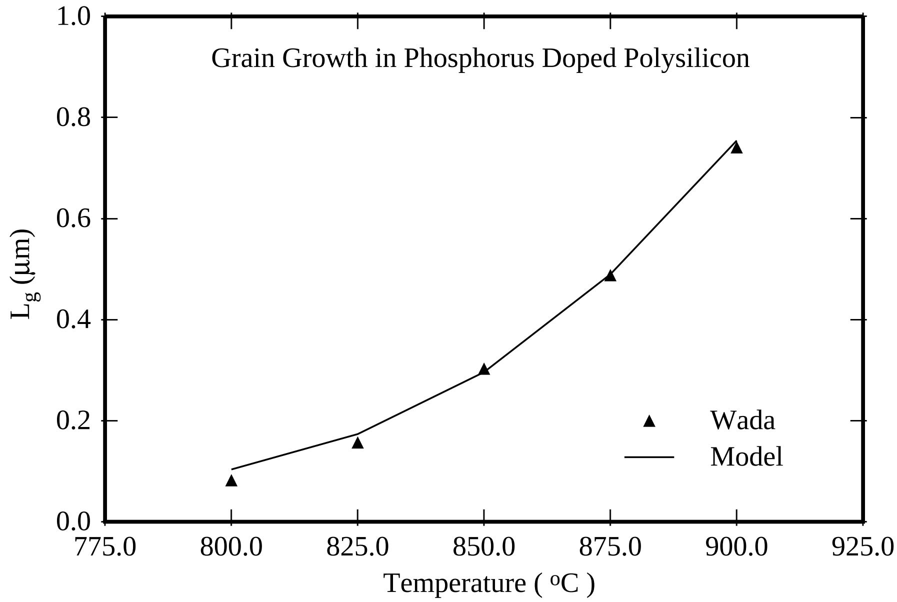

Figure 5.3: Comparison of model to experimental data for grain growth from Wada *et al.* Total phosphorus concentration in the polysilicon is 7.5×10^{20} and annealed for 1 h at different temperatures.

As discussed earlier, at high doping levels arsenic has been observed to behave differently than phosphorus regarding its effects on grain growth [13, 17]. Samples doped with arsenic at concentrations above solid solubility actually showed a reduction in grain growth rate while phosphorus continued to enhance grain growth rate. We have incorporated this effect in our model and the modified σ is of the form shown in Eq. 3.19. We have calibrated our model parameter C_r based on data from Angelucci *et al.* [17]. However, we had to modify M_1 and $K^{'}$ from that extracted from Wada *et al.* [16] and Kim and Thompson [11] to get good fits to this data. Since, the data from Wada *et al.* and Kim and Thompson are in the primary temperature range of interest to us (800°C - 1000°C), we use values of M_1 and $K^{'}$ derived from their data with the value of C_r obtained from the data of Angelucci *et al.* [17]. Fig. 5.5 shows a comparison of model with experimental data for grain growth vs. total doping concentration.

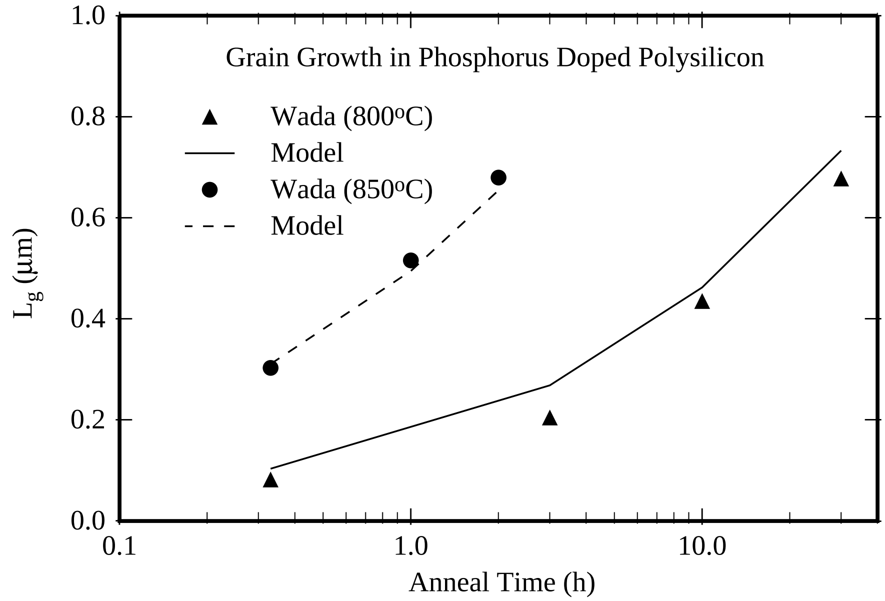

Figure 5.4: Comparison of model to experimental data for grain growth from Wada *et al.* [16]. Total phosphorus concentration in the polysilicon is 7.5×10^{20} and annealed for different times at 800°C and 850°C.

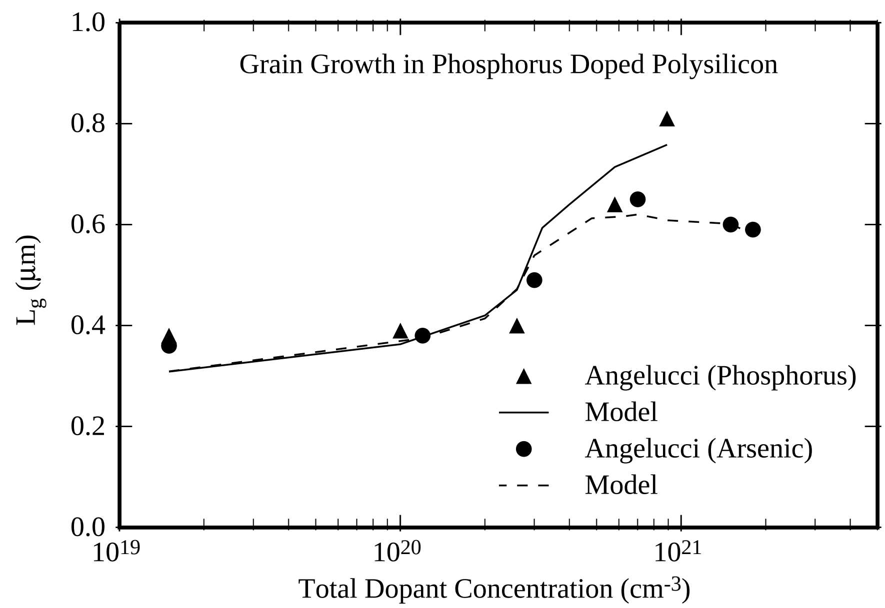

Figure 5.5: Comparison of model predictions of grain growth for varying dopant concentrations (arsenic and phosphorus) with data from Angelucci *et al.* [17]. Anneals for 1 h at 1050°C.

	$M_1\,\alpha\,\gamma_{\mathrm{gb}}$	$K^{'}$	C_{r} (cm^{-3})
Phosphorus	$4\times10^{14}\exp\left(\frac{-4.2}{k\,T}\right)$	$2.5\times10^{4}\exp\left(\frac{-1.1}{k\,T}\right)$	∞
Arsenic	$4\times10^{14}\exp\left(\frac{-4.2}{k\,T}\right)$	$2.5\times10^{4}\exp\left(\frac{-1.1}{k\,T}\right)$	8×10^{21}

Table 5.2: Grain growth parameter values for arsenic and phosphorus.

	C^{ss} (cm^{-3})
Arsenic	$2.22\times10^{22}\exp\left(\frac{-0.47}{k\,T}\right)$
Phosphorus	$1.8\times10^{22}\exp\left(\frac{-0.4}{k\,T}\right)$

Table 5.3: Solid solubility values for arsenic and phosphorus from Nobili *et al.* [42].

5.3 Dopant Diffusion

The model discussed in Chapter 3 has been implemented in PEPPER [51] using the “dial-an-operator” mode. With the exception of diffusivity in grain boundaries ($D_{\mathrm{A}}^{\mathrm{gb}}$), all other parameter values are fixed based on experimental results as described in Sections 5.1 and 5.2, with parameter values given in Tables 5.1, 5.2 and 5.3. Solid solubility parameter values have been taken from Nobili *et al.* Fig 5.6 shows a comparison of RBS data from Swaminathan *et al.* [33] with simulation results for a 800$^{\mathrm{o}}$C, 6 h anneal for an initial grain size in the poly of 0.51 μm. As can be seen from the figure, the peak remains near the surface due to the low diffusivity at low temperature and also due to solid solubility effects. The reduction in the peak from the as-implanted profile is because of dopant transfer from the grain interiors to the grain boundaries followed by fast diffusion along the grain boundaries deep into the film. This fast diffusion in the grain boundaries gives rise to the tail region of the profile. This figure also illustrates the grain and the grain boundary concentrations as a function of depth. It can be clearly seen that in the peak region of the profile much of the dopants is still in the grain due to most of the implant being in the grains (because grain boundary volume is typically only ~2% of the total polysilicon volume). However, deeper down into the polysilicon, most of the dopant is in the grain boundaries. Also, near the peak region there is a dip in the concentration within the grain boundaries. This is a result of the considerable grain growth occurring in this region. As the grains grow larger, the total grain boundary volume decreases and thus the concentration in the grain boundary drops. As discussed earlier, grain growth increases with dopant concentrations and so is maximum near the peak region of the profile.

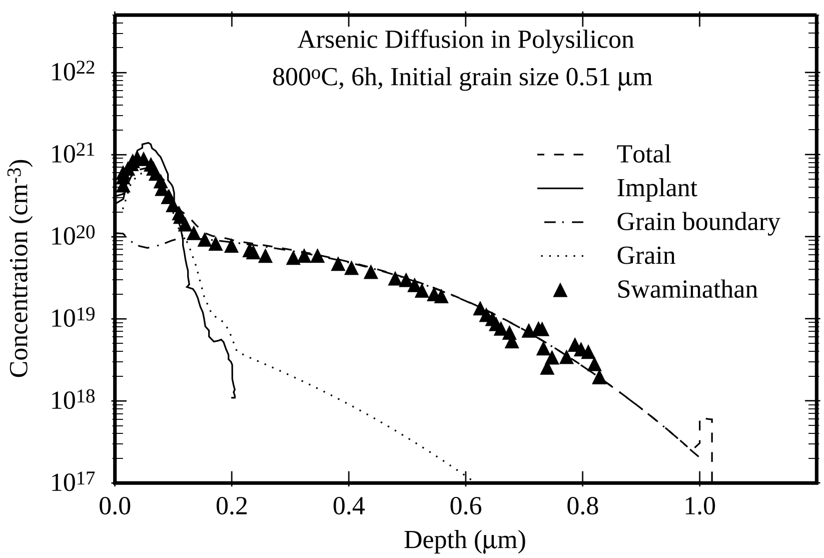

Figure 5.6: Comparison of model predictions with RBS data for a 800°C, 6 h anneal with initial grain size in poly being around 0.51 μm. Also shown are the grain and grain boundary components of the dopant profile. Data from Swaminathan *et al.* [33].

The other important feature to be noted in this figure is the peak in the dopant profile at a depth of 1.0 μm. The polysilicon/substrate interface lies at this point and it has been experimentally observed that dopants preferentially segregate to this interface [30]. However, the thickness of this interface region has been increased to account for SIMS broadening.

Fig. 5.7 shows values of k_D for arsenic and phosphorus evaluated for the same value of $\sqrt{D_{\mathrm{A}}^{\mathrm{g}}\, t}$ at different temperatures. As phosphorus diffusivity is higher than that of arsenic, k_D is higher at all temperatures. It is also interesting to note that k_D dominates over k_V at all temperatures for arsenic, whereas they are comparable at low temperatures for phosphorus.

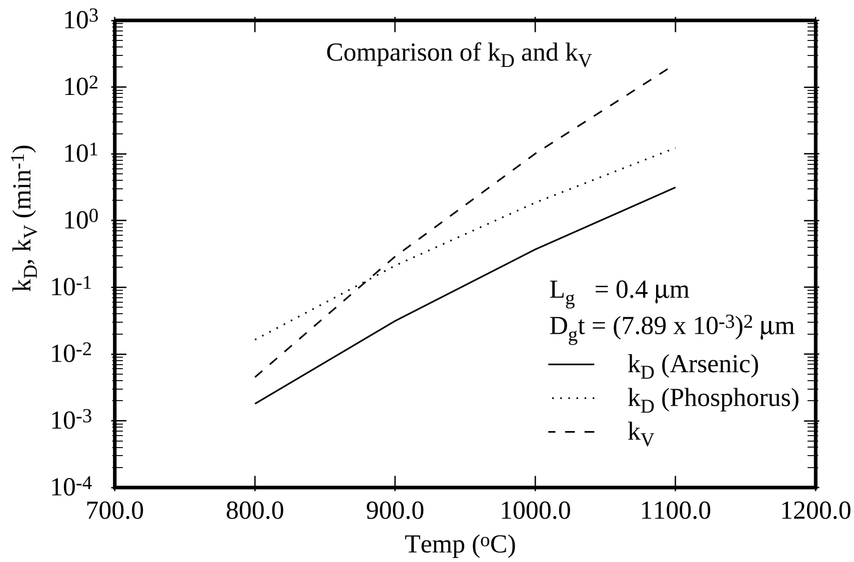

Figure 5.7: Comparison of estimates of the two different components of the transfer rate, k_D and k_V at different temperatures.

The post anneal dopant profiles in polysilicon are strongly dependent on the initial grain size of the polysilicon layer. For smaller grain size, the total grain boundary volume is more and grain growth is faster, so the percentage of dopants in the grain boundary is higher. As a result, the doping in the tail region of the profile which is dominated by the concentration in the grain boundary is higher for smaller initial grain sizes. This feature is captured well by our model and Fig 5.8 illustrates the dependence of the profiles on grain size.

This model is also able to do a good job of predicting the dependence of dopant

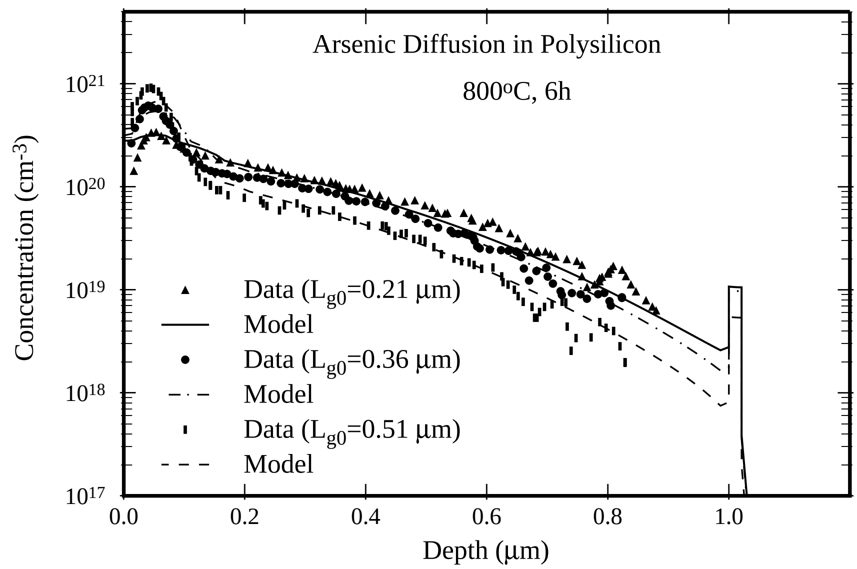

Figure 5.8: Comparison of model predictions with RBS data for varying initial grain sizes in the polysilicon for 800°C, 6 h anneals. Data from Swaminathan *et al.* [33].

profiles on the temperature as well as the time of the anneals. Fig 5.9 shows the comparison with SIMS profile for a 800°C, 5 h anneal and Fig 5.10 shows the temperature dependence of the profiles.

Fig. 5.11 shows the temperature ramp up and down that wafers went through in our 900°C anneal. This model is also able to predict diffusion during the ramp up and down as shown in Fig. 5.12.

Figs. 5.13 shows the comparison of model predictions for 900°C anneal for two different times. Again there is excellent agreement. In contrast, Fig. 5.14 shows comparison of model predictions for anneals at 1000°C for 5 s and 15 s. It can be clearly seen that the predicted grain boundary diffusivity is too low and the dopant incorporation into the grain boundaries in the peak region is insufficient. This suggests that the temperature during the RTA was actually significantly higher than 1000°C.

Following the arsenic implant, the upper region of the polysilicon layer is amorphized. This also leads to implant damage which has been found to cause transient enhanced diffusion (TED) in single crystal silicon. Also, the amorphized region rapidly

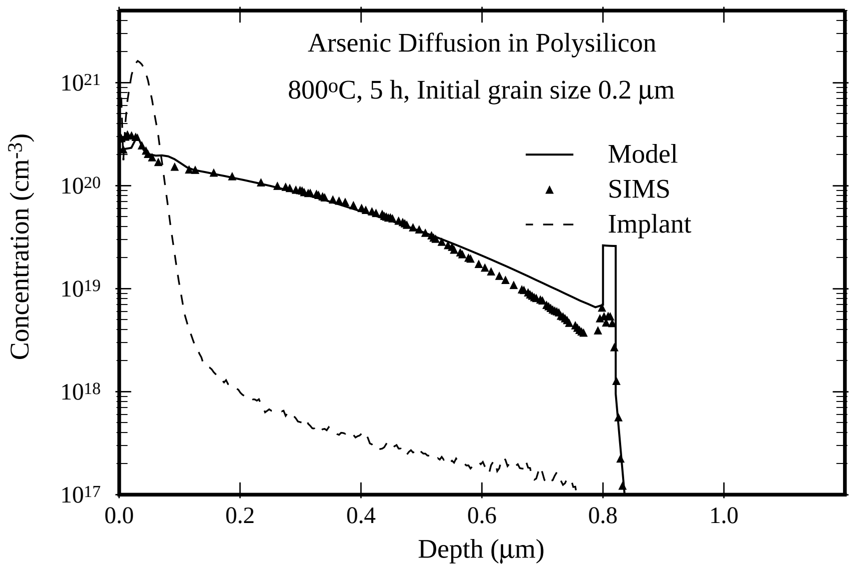

Figure 5.9: Comparison of model predictions with SIMS data for a 800°C, 5 h anneal.

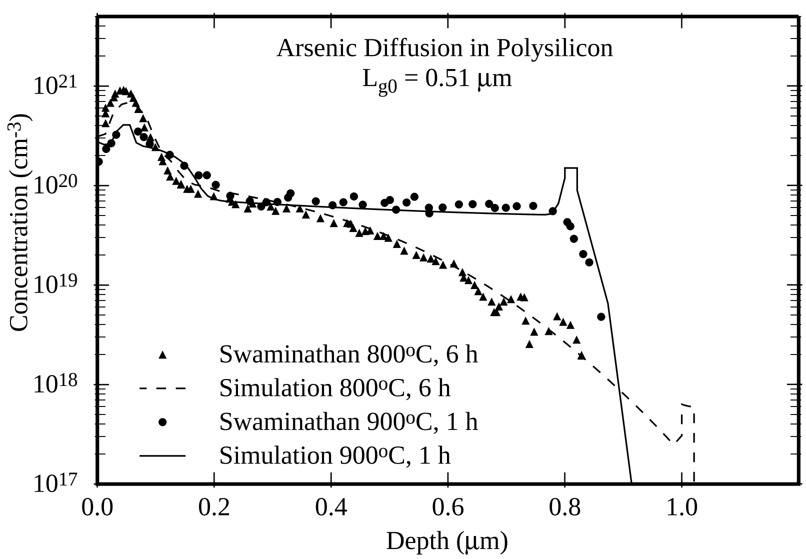

Figure 5.10: Comparison of model predictions with RBS data for 800°C, 6 h anneal and 900°C, 1 h anneal for the same initial grain size of 0.51 μm.

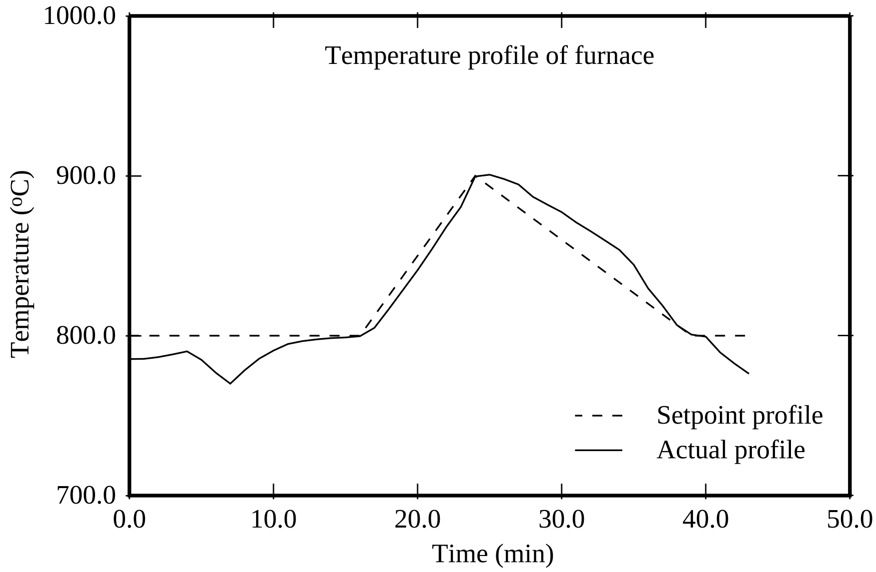

Figure 5.11: Actual temperature profile of furnace during a ramp up and down to (from) 900°C compared to the set point profile.

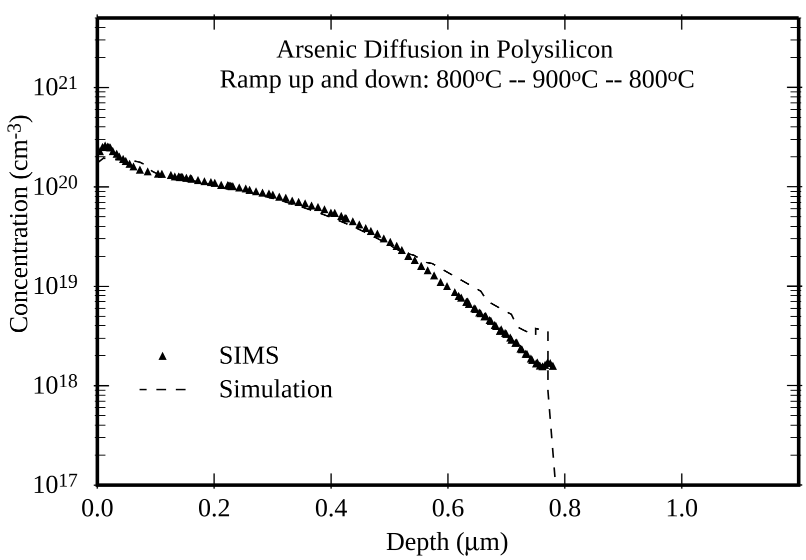

Figure 5.12: Comparison of model predictions to SIMS data for the temperature ramp up/down shown in Fig. 5.11.

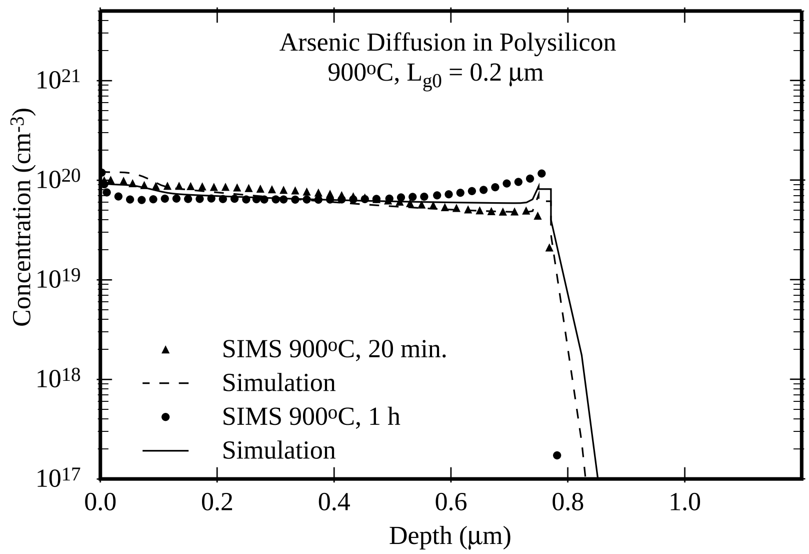

Figure 5.13: Comparison of model predictions for 20 min and 1 h anneals at 900°C with SIMS data from our experiments.

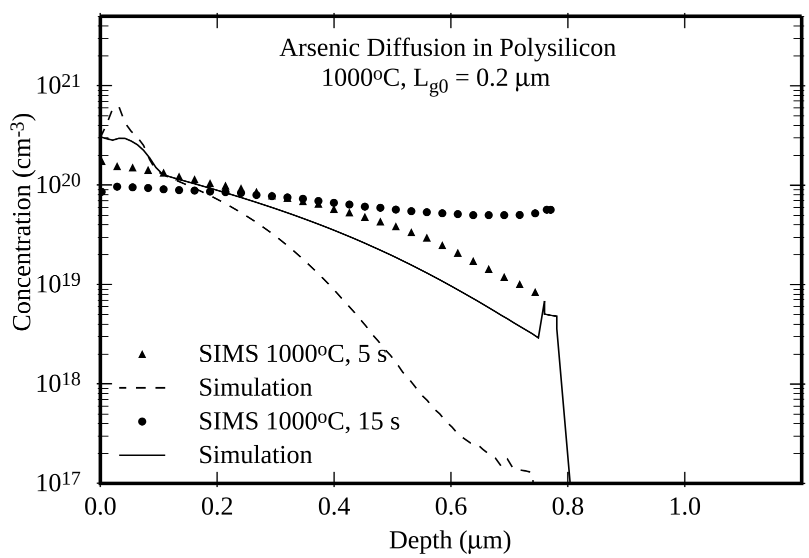

Figure 5.14: Comparison of model predictions to SIMS data for 5 s and 15 s anneals at 1000°C.

recrystallizes by epitaxial regrowth, dopants could be preferentially incorporated into grain boundaries during this process. However, Fig. 5.15 illustrates that a 800°C, 20 min anneal plus furnace push and pull can be well matched by a 800°C, 25 min anneal. This leads us to conclude that there is no significant TED effects or dopant incorporation for arsenic during epitaxial regrowth. It also validates our assumption that the grain structure regrows from the non-amorphized region.

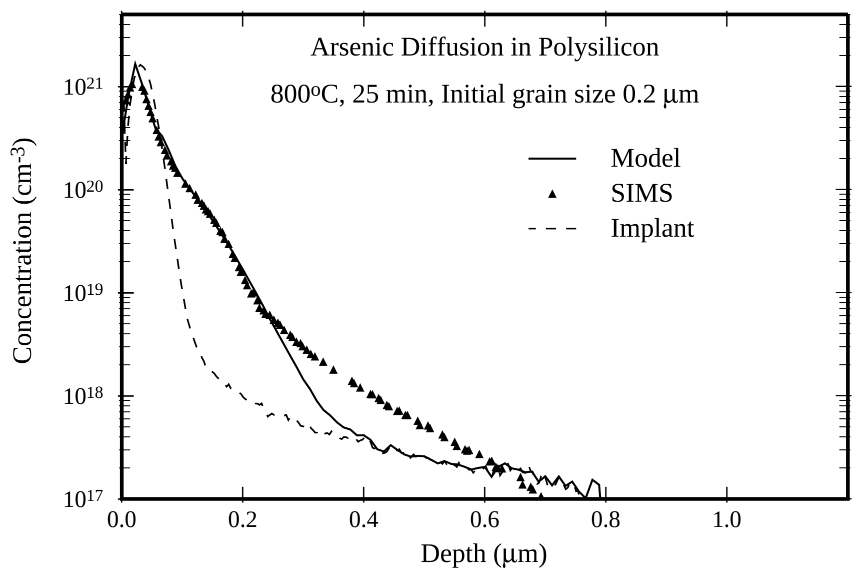

Figure 5.15: Comparison of model predictions for a 800°C, 20 min. plus furnace push and pull anneal with simulation for 25 min. at the same temperature.

	D_0 (cm^2 s^{-1})	D_- (cm^2 s^{-1})	C_{ref} (cm^{-3})
Grain	$8.0 \exp\left(\frac{-4.05}{k\,T}\right)$	$12.0 \exp\left(\frac{-4.05}{k\,T}\right)$	$1.01 \times 10^{21} \exp\left(\frac{-0.2}{k\,T}\right)$
Grain Boundary	$2.8 \times 10^6 \exp\left(\frac{-4.3}{k\,T}\right)$	$9.8 \times 10^5 \exp\left(\frac{-4.5}{k\,T}\right)$	–

Table 5.4: Grain and grain boundary diffusivity parameter values for arsenic.

Chapter 6

Conclusions and Suggestions for Future Work

In this work we have developed a model for dopant diffusion in polysilicon and have carried out experiments to characterize this model. To develop a predictive model for dopant diffusion in polysilicon, we need to understand the physical processes going on in polysilicon. The polysilicon microstructure consists of single crystal grains separated by regions of high defect concentrations called grain boundaries. Diffusivity within these grain boundaries is about 4 orders of magnitude higher than in bulk silicon. The grains grow in size when annealed at high temperatures and the growth rate is dependent on the Fermi level.

Four different transport mechanisms go on inside polysilicon: Diffusion of dopants through the grain interiors, diffusion along the grain boundaries, lateral diffusion of dopants from the grain interiors to the grain boundaries, and segregation of dopants to the grain boundaries. Besides these four processes, as the grains grow, grain boundaries sweep across dopant rich grain interiors and pick up dopants.

We have incorporated all these physical processes in a two stream model which divides the dopant into grain concentration and grain boundary concentration, coupled together by dopant transfer from one stream to the other. A model for dopant segregation to the grain boundaries has been developed which includes effects of saturation of grain boundaries as well as the grain size dependence. A model [11] for grain growth has been extended to account for the effects of finite film thickness and heavy doping. To ensure the physical basis of the model, parameters have been extracted from a large range of experimental results for application to prediction of dopant diffusion profiles.

Simulations have been carried out for various different times, temperatures as well as initial grain sizes in the poly and compared to experimental results. From these comparisons, it is evident that our model does a very good job of predicting dopant diffusion under various anneal conditions. Investigation of the time dependence of profile evolution lead to the conclusion that TED effects as well as dopant incorporation during epitaxial regrowth following amorphization during implants, is negligible for arsenic.

Continuation of this work would be to develop a 3D model based on these lines. The diffusion equations can be easily transformed to incorporate 3D effects, but grain growth requires assumption about grain orientation in non-planar structures. Also, we found substantial disagreement among measurements of polysilicon grain growth and a consistent set of experimental observations would greatly aid the further development of a quantitative model.

Bibliography

[1] E. G. Lee and J. J. Kim, "Investigation of microstructure and grain growth of polycrystalline silicon deposited using silane and dislane," *Thin Solid films* **226**, pp 123-128 (1993).

[2] E. Ibok and S. Garg, "A characterization of the effect of deposition temperature on polysilicon properties," *J. Electrochem. Soc.* **140**(10), pp 2927-2937 (1993).

[3] X. Ren, M. C. Ozturk, J. J. Wortman, B. Zhang, D. M. Maher and D. Batchelor, "Deposition and characterization of polysilicon films deposited by rapid thermal processing," *J. Vac. Sci. Technol. B* **10**(3), pp 1081-1086 (1992).

[4] K. Park, S. Batra, S. Banerjee, G. Lux and R. Manukonda, "Diffusion of As and B in polysilicon/single-crystal silicon systems," *Mat. Res. Soc. Symp. Proc.* **182**, pp 141-146 (1990).

[5] T. V. Rodionova, V. G. Kobka and N. G. Nakhodkin, "Growth of grains in polycrystalline films of silicon during annealing," *Sov. Phys. Crystallogr.* **33**(5), pp 715-718 (1988).

[6] A.R.Sitaram, S. P. Muraraka and T. T. Sheng, "Grain growth in boron doped LPCVD polysilicon films," *J. Mater. Res.* **5**(2), pp 360-364 (1990).

[7] J. P. Carrejo, T. Thundat, L. A. Nagahara, S. M. Lindsay and A. Majumdar, "Scanning tunneling microscopy investigations of polysilicon films under solution," *J. Vac. Sci. Technology B* **9**(2), pp 955-959 (1991).

[8] D. Bisero, "SEM Overestimation of the mean grain size of chemically etched polycrystalline silicon films," *Materials Letters* **18**, pp 215-217 (1994).

[9] S. Batra, K. H. Park, S. K. Banerjee, "Effect of Grain Microstructure on P Diffusion in Polycrystalline-on-Single Crystal Silicon Systems," *J. Electronic Materials* **21**(2), pp 227-231, (1992).

[10] S. Kalainathan, R. Dhanasekaran and P. Ramasamy, "Grain growth mechanism in boron doped polycrystalline silicon," *J. Electronic Materials* **19**(10), pp 1135-1139 (1990).

[11] H. J. Kim and C. V. Thompson, *VLSI Publications of MIT* **VLSI Memo** (87-376), (1987).

[12] H. J. Kim and C. V. Thompson, "Compensation of grain growth enhancement in doped silicon films," *Appl. Phys. Lett.* **48**(6), pp 399-401 (1986).

[13] L. Mei, M. Rivier, Y. Kwark and R. W. Dutton, "Grain-growth mechanisms in polysilicon," *J. Electrochem. Soc* **129**(8), pp 1791-1795 (1982).

[14] H. Puchner and S. Selberherr, "An advanced model for dopant diffusion in polysilicon," *IEEE Trans. on Electron Dev.* **42**(10), pp 1750-1754 (1995).

[15] H. J. Kim and C. V. Thompson, "The effects of dopants on surface- energy-driven secondary grain growth in silicon films," *J. Appl. Phys.* **67**(2), pp 757-767 (1990).

[16] Y. Wada and S. Nishimatsu, *J. Electrochem. Soc.* **125** pp 1419 (1978).

[17] R. Angelucci, M. Severi, and S. Solmi, *Mater. Chem. Phys.* **9**, pp 235 (1983).

[18] B. Cunningham and D. Ast, "Grain boundaries in semiconductors," *Mater. Res. Soc. Proc.* edited by H. J. Leamy, G. E. Pike and C. H. Seager **21** (1981).

[19] H. Ichinose, Y. Tajima and Y. Ishida, “Grain boundary structure and related phenomena,” *Proc. Japan inst. Metals. Int. Symp.* **253**, (1985).

[20] D. A. Smith and T. Y. Tan, “Grain boundaries in semiconductors,” *Mater. Res. Soc. Symp. Proc.* edited by H. J. Leamy, G. E. Pike and C. H. Seager,**249** (1982).

[21] M. M. Mandurah, K. C. Saraswat and T. I. Kamins, *J. Electrochem. Soc.* **126**, 1019 (1979).

[22] T. I. Kamins, *J. Appl. Phys.* **42**, 4357 (1971).

[23] Y. W. Seto, *J. Appl. Phys* **46**, 5247 (1975).

[24] M. E. Cowher and T. O. Sedgwick, *J. Electrochem. Soc.* **119**, 1565 (1972).

[25] A. L. Fripp and L. H. Slack, *J. Electrochem. Soc.* **120**, 145 (1973).

[26] M. M. Mandurah, K. C. Saraswat and T. I. Kamins, “Arsenic segregation in polycrystalline silicon,” *Appl. Phys. Lett.* **36**(8), pp 683-685 (1980).

[27] M. M. Mandurah, K. C. Saraswat, C. R. Helms and T. I. Kamins, “ Dopant segregation in polycrystalline silicon,” *J. Appl. Phys.* **51**(11), pp 5755-5763 (1980).

[28] E. Demirlioglu, *Stanford Electron. Labs. Tech. Rep. G502-10*,Stanford, CA, Dec. 1988.

[29] A. D. Sadovnikov, “One-dimensional modeling of high concentration boron diffusion in polysilicon-silicon structures,” *Solid-State Electronics* **34**(9), pp 969-975 (1991).

[30] S. Luning and J. D. Plummer, “Experimental characterization of arsenic behavior in poly/single-crystal silicon system,” *SRC Pub C93094* (1993).

[31] C. Gontrand, A. Merabet, B. Semmache, S. Krieger-Kaddour, C. Bergaud, M. Lemiti, D. Barbier and A. Laugier, "Co-diffusion of As and B in and from polysilicon during rapid thermal annealing," *Semicond. Sci. Technol.* **8**, pp 155-162 (1993).

[32] C. Gontrand, M. Lemiti, C. Dubois, S. Kaddour, E. Ehret and D. Barbier, "Redistribution of As and B co-implanted in polysilicon/monocrystalline emitter structures during rapid thermal annealing," *Mat. Res. Soc. Symp. Proc.* **224**, pp 341-346 (1991).

[33] B. Swaminathan, K. C. Saraswat, R. W. Dutton and T. I. Kamins, " Diffusion of arsenic in polycrystalline silicon," *Appl. Phys. Lett.* **40**(9), pp 795-798 (1982).

[34] M. Arienzo, Y. Komem and A. E. Michel, "Diffusion of Arsenic in Bilayer Polycrystalline Silicon Films," *J. Appl. Phys.* **55**(2), pp 365-369, (1984).

[35] A. D. Sadovnikov and A. V. Tchernyaev, "Two-dimensional model of impurity diffusion in polysilicon-silicon structures," *Solid-State Electronics* **35**(2), pp 193-200 (1992).

[36] C. Hill and S. K. Jones, "Modeling diffusion in and from polysilicon layers," *Mat. Res. Soc. Symp. Proc.* **182**, pp 129-140 (1990).

[37] S. K. Jones and C. Hill, "Modeling dopant diffusion in polysilicon," *Simulation of Semiconductor Devices and Processes* **3**, pp 441- 449 (1988).

[38] F. Lau, " Modeling of polysilicon diffusion sources," *IEDM 90* pp 737-740 (1990).

[39] A. G. O'Neill, C. Hill, J. King and C. Please, "A new model for the diffusion of arsenic in polycrystalline silicon," *J. Appl. Phys.* **64**(1), 167 (1988).

[40] J. W. Cahn, "The impurity drag effect in grain boundary motion," *Acta Metallurgica* **10**, pp 789-798 (1962).

[41] S. T. Dunham and C. D. Wu, *J. Appl. Phys.* **78**, 2362 (1995).

[42] D. Nobili, “Properties of silicon,” *EMIS Datareview N.* **4**, pp 394 (1988).

[43] L. Gonzo, A. Lui and D. Bisero, “Scanning tunneling microscopy investigation of phosphorus-doped polycrystalline silicon films,” *Materials Letters* **18**, pp 50-56 (1993).

[44] M. Hane and S. Hasegawa, “Dynamic-clustering and grain-growth kinetics effects on dopant diffusion in polysilicon,” *IEICE Trans. Electron.* **E77-C**(2), pp 112-116 (1993).

[45] S. K. Jones and A. Gerodolle, “2D process simulation of dopant diffusion in polysilicon,” *COMPEL - The International Journal for Computation and Mathematics in Electrical and Electronic Engineering* **10**, pp 401-410 (1991).

[46] T. I. Kamins, J. Manoliu and R. N. Tucker, *J. Appl. Phys.* **43** pp 83 (1972).

[47] D. Kruger, P. Gaworzewski, R. Kurps and J. Schlote, “Phosphorus segregation at polysilicon-silicon interfaces from in situ P spike-doped silicon films,” *Semicond. Sci. Technol.* **10**, pp 326-331 (1995).

[48] N. Lifshitz, “Solubility of implanted dopants in polysilicon : phosphorus and arsenic,” *J. Electrochem. Soc.* **130**(12), pp 2464-2467 (1983).

[49] A. Merabet and C. Gontrand, “Dopant redistribution during rapid thermal annealing in a self-aligned polysilicon emitter bipolar structure compatible with a complimentary metal-oxide-semiconductor technology,” *Phys. Stat. Sol. (a)* **145**(77), pp 77-88 (1994).

[50] L. Mei and R. W. Dutton, “A process simulation model for multilayer structures involving polycrystalline silicon,” *IEEE Trans. on Electron Dev.* **ED-29**(11), pp 1726-1734 (1982).

[51] B. Mulvaney, W. B. Richardson and T. L. Crandle, "PEPPER - a process simulator for VLSI," *IEEE Trans. on Comp. Aided Des.* **8**(4), pp 336-349 (1989).

[52] K. Park, S. Batra, S. Banerjee, G. Lux and T. C. Smith, " Analysis of ion-implanted amorphous and polycrystalline silicon films as diffusion sources for ultrashallow junctions," *J. Appl. Phys.* **70**(1), pp 1397-1404 (1991).

[53] H. Puchner and S. Selberherr, "Dynamic grain-growth and static clustering effects on dopant diffusion in polysilicon," *International Workshop on Numerical Modeling of Processes and Devices for Integrated Circuits, NUPAD V* pp 109 -112 (1994).

[54] C. M. Ransom, T. N. Jackson, J. F. Degelormo, D. Kotecki and C.Graimann and D.K.Sadana "Arsenic gas-phase doping of polysilicon," *J. Vac. Sci. Technol. B* **12**(3), pp 1390-1393 (1994).

[55] H. Ryssel, H. Iberl, M. Bleier, G. Prinke, K. Haberger and H. Kranz, *J. Appl. Phys.* **24**, pp 197 (1978).

[56] H. Schaber, R. V. Criegern and I. Weitzel, "Analysis of polycrystalline silicon diffusion sources by secondary ion mass spectroscopy," *J. Appl. Phys.* **58**(11), pp 4036-4042 (1985).

[57] S. P. Chen, J. D. Kress, A. F. Voter and R. C. Albers, "Modeling of Si grain boundaries and vacancies", *Process Phys. and Modeling in Semiconductor Technology*, edited by G. R. Srinivasan, C. S. Murthy and S. T. Dunham (1996)

[58] K. Srikrishna, M. Moinpour and B. Landau, "Polysilicon/silicon interfaces: effect of processing parameters on physical and electrical properties," *Mat. Res. Soc. Symp. Proc.* **262**, pp 713-718 (1992).

[59] A. Sultan, S. Bhattacharya, S. Batra and S. Banerjee, "Boltzmann- Matano analysis based model for boron diffusion from polysilicon into single crystal silicon," *J. Vac. Sci. Technol. B* **12**(1), pp 391-394 (1994).

[60] K. Suzuki, Y. Yamashita, Y. Kataoka, K. Yamakazi and K. Kawamura, "Segregation coefficient of boron and arsenic at polycrystalline silicon/SiO_2 interface," *J. Electrochem. Soc.* **140**(10), pp 2960-2964 (1993).

[61] B. Swaminathan, E. Demoulin, T. W. Sigmon, R. W. Dutton and R. Reif, "Segregation of arsenic to the grain boundaries in polycrystalline silicon," *J. Electrochem. Soc* **127**(10), pp 2227-2229 (1988).

[62] C. V. Thompson and H. I. Smith, "Surface-energy-driven secondary grain growth in ultrathin ($\langle$ 100nm) films of silicon," *Appl. Phys. Lett.* **44**(6), pp 603-605 (1984).

[63] C. V. Thompson, "Secondary grain growth in thin films of semiconductors: theoretical aspects," *J. Appl. Phys.* **58**(2), pp 763-772 (1985).

[64] K. Tsukamoto, Y. Akasaka and K. Horie, *J. Appl. Phys.* **48** pp 1815 (1977).